Index of contents

Abstract

Regeneration is a process that restores structure and function of tissues damaged by injury or disease. In mammals complete regeneration is often unsuccessful, while low phyla animals can re-grow many parts of their body after amputation. Cephalopod molluscs, and in particular *Octopus vulgaris*, are well known for their capacity to regenerate their arms and other body parts, including central and peripheral nervous system. To better understand the mechanism of recovery following nerve injury in this species we investigated the process of axon regrowth and nerve regeneration after complete transection of the *Octopus* pallial nerves. This injury induces scar formation and activates the proliferation of hemocytes which invade the scar. Hemocytes appear involved in debris removal and seem to produce factors that foster axon re-growth. Connective tissue is involved in driving regenerating fibers in a single direction, outlining for them a well-defined pathway. Injured axons are able to quickly re-grow thus to restoring structure and function.

Aims and project outline

Regeneration is a fascinating topic which has interested scientists, philosophers and even common people since antiquities. It has long been explored in many taxa, in vertebrates and invertebrates, when finally in the eighteen-century naturalists started a true investigation of the phenomenon (for a review Dinsmore book).

Among mollusks, cephalopods also showed the ability in regenerating lost parts and in recovering its function, dragging the attention of many researchers for over a century. Indeed, since 1856, when the first paper on octopods arm regeneration was published, many others followed leading to the understanding of the impressive ability of this class in regenerating appendages, cornea, nervous system and even brain, although the machinery involved still remains obscure. Although all the findings and the understanding that cephalopod could greatly contribute in deciphering biological pathways that may result beneficial in supporting translation towards adult mammalian regeneration, in the late twentieth century, research on cephalopods suffered a sudden halt. Regenerative studies on other species, in particular in planarians, nematodes, salamanders, axolotls and even mammals, instead, kept going on, heading to the development of advanced techniques and methods that allowed unravelling, at least in part, pathways involved in the complex machinery of the regenerative phenomenon.

I proposed to use the regeneration of the pallial nerve of *Octopus vulgaris* as an easy model to study the mechanisms involved in the regenerative processes of the nervous tissue in invertebrates. The pallial nerve provides an exceptional example to study nerve regeneration, because: ***i.*** Regeneration is always very quick and efficient. ***ii.*** It is immediately possible to evaluate loss and regain of function by simply evaluating breathing movements and skin patterning in the mantle of the animal. ***iii.*** Each animal has a pair of nerves, one on each side of the mantle, allowing the same animal to serve as experimental and control; ***iv.*** The same nerve can be lesioned several times providing almost complete regeneration at each instance; ***v.*** The majority of the cell soma of axons in the pallial nerve is inside the brain, but others in the ganglia at periphery. Both can regenerate, allowing a comparison of regeneration ability of the two 'systems'; ***vi.*** Octopus represents a "simpler" animal compared to vertebrates; however, regeneration/degeneration phenomena following lesion are similar to those happening in higher vertebrates (Wallerian degeneration).

The main aims of this project proposed were:

- Evaluation of the time needed to obtain full nerve regeneration and of the functional integrity of the regenerated nerve.
- Identification of the main morphological, cellular and molecular processes involved.

- Identification of RAGs and epigenetic genes involved in the process.
- Pharmacological ablation of deacetylases and demethylases using inhibitors and evaluation of recovery time in the presence of these inhibitors.
- Identification of bivalent chromatin in regenerating and non-regenerating tissues.

Despite challenging, majority of the objectives were achieved, leaving behind some points:

- The evaluation of the functional integrity of the regenerated nerve was not obtained through electroneurography (ENoG), as meant to be, but through the evaluation of function recovery. I have to say that electrophysiological studies were performed in the past and had already proved that the nerve re-establish its connections.
- Pharmacological ablation of deacetylases and demethylases using inhibitors and evaluation of recovery time in the presence of these inhibitors.
- Identification of bivalent chromatin in regenerating and non-regenerating tissues.

However one important achievement, that was not present in the original project, was obtained:

- The identification of new markers, imaging techniques and tracing methods

which can be beneficial for the whole community performing research in cephalopods.

Past and present of cephalopod regeneration

Regeneration in cephalopods has interested researchers since 1856, when Steenstrup first described the ability of some members of this class to regrow lost appendages. This extraordinary feature is widespread among many species of octopuses, squids and cuttlefishes, being detected also in the fossil cephalopod subclass of Ammonoidea. Here we will review past and present knowledge of the regenerative capabilities of cephalopods, which are not limited to arms and tentacles but interests several tissues, showing also evidence of axon re-growing in the central nervous system.

Wound healing

Skin, fin and arm damages are extremely common in cephalopods due to several reasons: autophagy, autotomy, fungal and bacterial lesion, capture, transportation (Hanlon et al., 1984; Ford, 1992; Budelmann, 1998, Florini et al, 2011; Bush, 2012). All these structures are able to heal quite quickly and to restore the temporarily lost function.

Wound healing has been investigated in cephalopods especially as the first step of regeneration occurring after arm lesion (Lange, 1920; Feral, 1978; Feral, 1979). A deep investigation on this topic was undertaken in *S. officinalis* (Feral, 1988) highlighting the importance of wound healing as essential phenomenon for correct arm regeneration in this species. The healing process is dependent on several variables: temperature, position of the injury (distal portion of the arm compare to proximal), species, animal age, state of health, size and source. It was reported to takes as less as 24 hours (Lange, 1920); however, Feral (1988) reported that the complete healing requires around 5 days at a temperature between 14 and 19°C and around two weeks at 10°C.

Very recently in *O. vulgaris* two populations of healers were identified on the basis of healing speed: “faster” and “slower” healer (Shaw, 2016). Six hours post-lesion are indeed sufficient for the first group to cover 80% of the wound, while the second population covered only 50-60% of the lesion.

Soon after lesion, no bleeding was detected even though vessels in the arm were damaged and the axial nerve protrudes from the wound (Lange, 1920; Feral 1978). The edges of the wound start contracting to close the lesion. A few hours after lesion (around 6h later), amoebocytes rush to the lesion, invading nerve, connective tissue and muscles and changing shape from the spherical circulating type to a spindle shaped extravascular ones. The highest increase is blood cells occurs between day one and three, and allows the formation of a pseudoclot of usually five layers in 36 hours. Then, at day five the number of amoebocytes decreases till day seven which correspond to the end of wound healing process. Fibrous materials were also identified: a first type covering nerve cord and muscles and forming a net among amoebocytes in the scar and a second one, made of collagen fibers, into the hypodermis. Agglutinated amoebocytes form the scar which was eventually invaded by collagen fibers (the latter probably produced by the blastema). The

maximum increase in collagen was obtained 48h after amputation, decreasing with time to the initial level at the end of cicatrization. A few hours after lesion, epidermis detaches locally, and 24h later epithelial cells spread over the wound. These cells change in shape, from cuboidal to flat, do not proliferate and remain functional during spreading, which required 3-5 days (Feral, 1988). Hemocytes have been unanimously considered the main contributors and supporters of the healing process. However, a role for muscle cells (through de-differentiation) has also been recently proposed (Shaw et al, 2016)

The process of wound healing has also been investigated after "standard" injury of mantle skin in *E. cirrhosa* through a biopsy punch (Polglase, 1983; Bullock, 1987). Skin healing is fundamental to protect cephalopods against pathogens that would more easily infiltrate the damaged structure, often causing death of affected animals (Hanlon, 1984).

The first 12 hours post-wounding are characterized by infolding of the epidermis close to the wound and muscular contraction. The wound appears initially disorganized and damaged blood vessels give rise to the formation of hemorrhagic areas. Necrotic fibroblasts appear 1hpw and greatly increase 3hpw. Epidermal curvature required at least 30 min to start, but at 3hpw contraction of the skin greatly reduced the wound. Injured animals also showed stroking or holding of the wound.

Five hpw epidermal cell and hemocytes increased in number at wound site. The latter occurs through diapedesis and accelerates around 12 hpw, concomitant with swelling of the central area of the wound. 24 hpw hemocytes were observed to penetrated deeper in the wound and transform their shape, from a classical round to a fusiform one, covering the entire wound at around 30 hpw, providing a dermal plug.

Epidermal migration, which becomes extremely evident at 48 hpw, cleaved a passage thorough the hemocytes plug and cell activity decreased. 80 to 96 hpw is characterized by an increase in cellular organization, as hemocytes align themselves in stratified layers which assume the appearance of fibroblast cell types. Although closure was complete 120 hpw, the wound assumed the structure of uninjured epidermis only 50 days pw as cells had to undergo shape transformation and depth increasing. Pigmented cells did not appear to regenerate. Slow continuous contraction of the wound still occurs even up to 150 days pw. (Polglase, 1983).

Bacterial infection (i.e. *Vibrio tubiashii*) is able to extensively affect skin wound healing in *E. cirrosa*. In particular, infection inhibits muscular contractions of the wound at early stages and it induces a greater response of hemocytes, the latter often appearing to be necrotic. They also form a secondary dermal plug that limit the infection. Infection appears to delay epidermal migration and results in incomplete closure of the wounds (Bullock, 1987).

Appendage regeneration

Cephalopods appendages are extremely flexible muscular hydrostat missing fluid-filled cavities (characteristics of the hydrostatic skeleton of many invertebrate), and hard skeletal supports (Kier and Smith, 1985; Smith and Kier, 1989; Kier, 2016). Octopods are provided with eight arms, while

Decapods possess in addition a couple of tentacles. Cephalopod appendages are basically made of a nerve cord running in the central axis, surrounded by a three-dimensional array of muscle fibers; a single or double row of suckers (depending on the species) is present on the entire ventral surface of arms while on tentacles they are clustered only in the end part, which is named club. Suckers are very versatile organs which are singly connected to the axial nerve cord through a ganglion. This organization allows movements, maintenance of the posture, prey capture and manipulation (Graziadei, 1971; Kier 1982; Kier 2016). These extraordinary appendages are able to perform very fine and complex movements which have inspired the construction of robotic arms and soft OCTOPUS robots (Margheri et al. 2012; Cianchetti et al 2015).

A particular feature of male cephalopod's arm is the hectocotylus, which is the copulatory arm utilized to transfer spermatophores to the female; this arm is indeed equipped with a longitudinal groove for the passage of sperm; the latter is delivered to the seminal receptacle of females where it can be stored for a time period before egg fertilization.

Arm damage in cephalopods is extremely common in the wild. It was reported that 51% of *O. vulgaris* captured in the Bay of Naples (Florini et al., 2011) and 26% of the Pacific pygmy octopus, *Octopus digueti,* from Cholla Bay showed damage of one or more arms (Voight, 1992). In both cases, dorsal arms were more affected compared to ventral ones.

Although the ability of cephalopods to survive arm and tentacles loss is well-known since many centuries, being described by Aristotle in the 3rd century before Christ in his Historia de Animalibus, the first manuscript reporting cephalopod arm regeneration is dated 1856, where Steenstrup, describing the main structural features of the arms and the hectocotylus of several cephalopod species, focuses also on the ability of Octopoda to regenerate arms lost in copulation, injured or bitten off by predators. In addition, he pointed out the inability of Decapoda to regrow lost appendages, attributing them only the power of healing the wound.

The finding of some specimens of two squid species, *Loligo pealei* and *Ommastrephes illecebrosus*, with regenerating suckers, parts of tentacles or arms, allowed Verril (1881) to deny Steenstrup's statements on Decapoda, later also confirmed by many other findings. The 19 century was, indeed, characterized by the discovery of many new cephalopod species, many of which displaying regeneration (Verrill, 1882; Brock, 1886; Riggenbach, 1901) or arm dichotomy (Appellof, 1893; Parona, 1900; Hanko, 1913). However, all these papers were mainly descriptive of the finding of regenerating parts, but lacked experimental investigation. Lange (1920) started a detailed investigation, based on macroscopic observation and histological analysis, of the process of arm regeneration for three cephalopod species: *Octopus vulgaris*, *Eledone moschata* and *Sepia officinalis*. Above all, some statements are noteworthy: ***i***. arm regeneration can be dived into three stages: wound healing, tissue degeneration and renewal; ***ii.*** the whole process occurs through morphallaxis, as existing tissues rearrange, being responsible for the regeneration of the new tissues (with the exception of the dermal connective tissue); ***iii.*** proliferation is involved and cells seem to divide only through amitotic division, mitosis was never observed; **iv.** cuttlefish ability to regenerate lost appendages is stressed again, but it probably happens through "compensatory regulation" (namely development) of a rudimentary buccal arm rather than actual regeneration of the lesioned arm; v. the arm tip, which Lange claimed to be made of tissue in an undifferentiated

embryonic stage, requires less time to regenerate and form the embryonic blastemal compared to the time required if the lesion is made at the base of an arm, where tissues are more differentiated

Sucker re-innervation during arm regeneration was not covered by Lange, but this was matter of discussion of May's article in 1933. In this paper he supports Cajal neurotropic theory, the latter stating that nerve endings during embryogenesis and regeneration are attracted by chemicals produced by tissues that have to be innervated. This seems to be the case also for cephalopods were new forming suckers, in a regenerating arm, attract nervous fibers from the central nervous axis.

So far, majority of reports concerned regeneration of appendages in octopods, while information on decapods was still poor. The reasons ascribed for this lack of knowledge were the greater difficulties encountered in rearing decapods compared to octopods (Lange, 1920; Sereni and Young, 1932) and to a reduced frequency in arm or tentacles mutilation found for squids and cuttlefish (Lange, 1920; Adam, 1937). This last observation and some of Lange's assumptions were questioned by Aldrich and Aldrich (1968) who investigated, also in this case with solely macroscopical descriptions, over the finding of a specimen of giant squid *Architeuthis dux* with a regenerating tentacle. This study led the authors to disagree whit Lange assertions both about the frequency of regenerative phenomena and the way regeneration occurs in decapods, at least for *A. dux*, *L. pealei*, *I. illecebrosus* and *L. harveyi*. However, they did not completely refused the hypothesis of "compensatory regulation" speculating on the reporting of fishermen of some "eleven-armed squids", which apparently might be due to the presence of an injured arm and the corresponding growing rudimentary buccal arm.

Finally, between 1978 and 1979, also thanks to the improvements in breeding conditions for *S. officinalis,* Feral was able to conduct detailed studies on the phenomena occurring during arm regeneration in this species. Complete arm regeneration and functional recovery was obtained after experimental lesion in young *Sepia officinalis*, which required two and a half-three months (16°C). Regeneration was proven to be dependent on age, physiological state and water temperature, with adults being less able to regenerate or did not regenerate at all after healing during late autumn or winter, especially if water temperature fell below 14°C. Similar observations about regenerative abilities were also made in the *Sepiola atlantica*. Morphological observations (Feral, 1978) allowed identification of six stages of regeneration, while histological and cytological analysis brought to the identification of three phases (Feral, 1979) summarized below and in figure ?? __process___

Stage 1_ (From surgery to day seven). It is characterized by the protrusion of the central nervous axis and the spasmodic contraction of the wound's edge. A few hours after lesion one or two suckers close to the lesion move forward; they resume their normal position only two or three days later. Five to seven days are required for the epidermis to completely cover the wound.

Stage 2_ (From day five to fourteen). Due to swelling of the scar at the level of the nervous axis, a bud-shaped hemisphere appears at the injury site.

Stage 3_ (From day ten to twenty-one). It is characterized by the evolution of the regenerate toward a conical shape.

Stage 4_ **(From day seventeenth to twenty-fifth).** Rough suckers appear first on the ventral side of the stump close to the lesion and then on the regenerate.

Stage 5_ **(From day twenty-five to thirty-five).** Chromatophores appear gradually on the regenerate.

Stage 6_ **(Beyond day thirty).** The regenerate regains its functionality. It gets thicker, suckers become functional as well, and chromatophores increase in number, getting larger and darker.

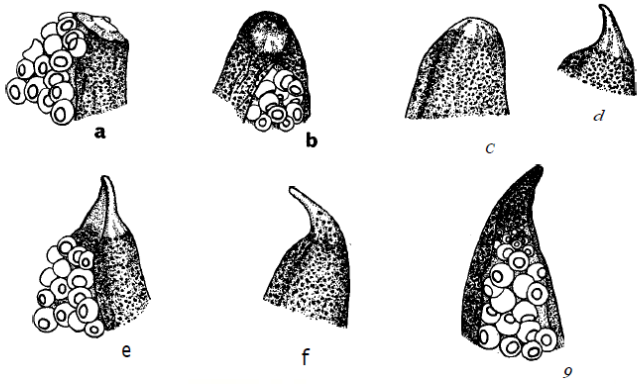

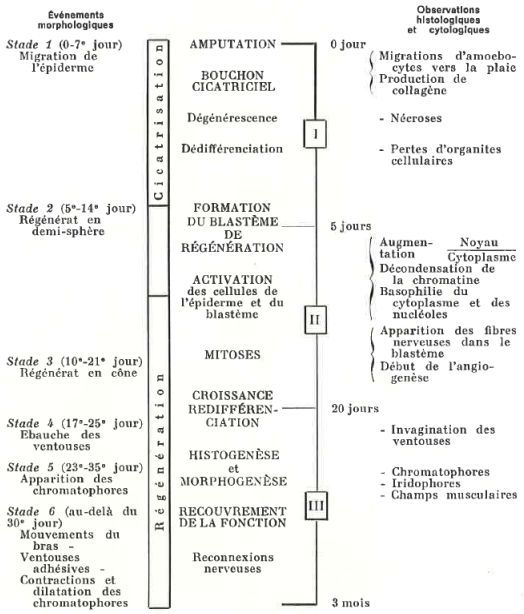

Phase I (corresponding to stage I- from day 1 to 7). It involves cicatrization, degeneration and dedifferentiation. Even though amoebocytes (blood cells) are unable to clot due to fibrin lack, they migrate to the injury and stick together preventing bleeding (pseudo-clot). Within 24 hours a fibrous cap is formed.

Degeneration of nerve cords, muscles and blood vessels close to the wound begins immediately after the section. Amoebocytes phagocytize nervous and muscular debris, while other blood cells lyse. This happens together with nerve fibers regeneration. Dedifferentiation occurs quickly after amputation and appears to involve all cell types close to the injury (but not epidermis), including amoebocytes. The blastema is formed mainly by dedifferentiated cells from tissues surrounding the wound, while epidermal cells keep most of their features. Mitotic cells were not observed in this phase neither in the epidermis nor in the blastema.

Phase II (corresponding to the end of stage 1, stage 2 and part of stage 3 – from day 5 to 20) represents the starting point of regeneration where blastema formation, cellular activation and regenerate growth occur. Blastema is made of dedifferentiated cells which in the first ten days increase in number, although no mitotic event is recorded; at a certain point in this phase, cells activate and start changing their appearance. Growing of the regenerate starts at this point, nervous fibers invade the blastemal. Mitosis starts at the end of the second week. The brachial artery progresses inside the blastema together with the axial nerve cord. The epidermis appears multilayered but, at the end of the third week, it is again simple.

Phase III (corresponding to the end of stage 3, stage 4, 5 and recovery of function– from day 20 to the third month): in this phase there is arm re-growing and differentiation. After the third week mitosis is reduced and cells differentiate. Differentiation occurs via concentric field around the nerve cord. The nervous system differentiate first: primarily the fibers extending the cerebro-brachial tract penetrate into the blastema; ganglionic layer formed by dividing neuroblasts, appears afterwards. Neuropil is edified gradually issued by neuron fibers. Glial cells support nerve fibers during regeneration. Around day 20 they start to divide and follow axons progress. They also contain large mitochondria which also appear to divide.

The axial nervous system, the brachial artery and “epineuraux” muscles differentiate jointly. Intrinsic longitudinal muscles appear visible at the 20^{th} day, together with the collagen that limits it toward the outside; later, extrinsic longitudinal muscles appear followed by transversal muscles. Muscles of the suckers (acetabular) also form by the third week by proliferation of central fascicles. During invagination the sucker chambers, muscle cells form first one, then several, parallel layers. These cells form the radial muscles and sphincters. Following suckers also acetabulo-branchial muscles differentiate. Suckers innervation occurs only at later stages, when suckers are completely formed, around the 40^{th} day and become functional only three months after injury. The dermis appears to originate from amoebocytes.

Chromatophores are identified among fibroblasts before they actually appear on the skin thanks to the presence of pigmented grains. Around day 20 the cells of the dermis differentiate. Iridophores appears some days later (25^{th}-27^{th} day). At the beginning they are positioned without a specific orientation; later they arrange parallel to each other in the cytoplasm of the cell. Radial muscles of these organs differentiate when muscles form; however their innervation occurs later, indeed fibers from the median nervous axis start growing at the end of the third week, even though chromatophores and iridophores complete innervation occur between the second and third month after surgery.

The basal membrane of the epithelial cells appears at the moment of differentiation; it folds to form the draft of the suckers, then it invaginates forming the suction and adherent chambers. This occurs together with the appearing of the brachial vein into the regenerate.

Regeneration in *Sepia officinalis* is defined comparable to cephalopods octopods and other molluscs, and to some extent to Amphibian Urodeles. Some features to be highlighted: the role of amoebocytes which rush to the lesion site, impede bleeding and phagocytize cellular debris; dedifferentiation is necessaire for regeneration as it is identified as the only source of "regenerative" cells. The only other cell type involved in the process is amoebocytes which rush to the injury site, but this phenomenon stops before blastemal is formed.

It is difficult to identify cells involved in the dedifferentiation and re-differentiation, as they are only based on topographic cues. However, Feral suggests a possible dedifferentiation mechanism followed by cellular re-differentiation of amoebocytes into fibrocytes; the possibility that Cephalopods blood cells can differentiate in another cell type had already been proposed by Jullien et al. 1956.

Chromatophores and iridophores redifferentiate necessarily from the dedifferentiation of another cell type, probably an amoebocyte or a fibrocyte which can express different kind of potentiality as function of the position inside the blastemal (close to the epidermis) and of other cells.

The complex phenomenon of arm regeneration in *Sepia officinalis* appears to occur via epimorphosis for the epidermis (without dedifferentiation) and morphallaxis for the other tissues.

Amoebocytes are the only cells which rush to the lesion; however when this migration stops, the number of cells forming the blastemal keeps increasing, even though mitotic events are not observed. It is merely local cellular reorganization. In the lesion, damaged cells degenerate and are removed; the other ones dedifferentiate losing their peculiar features and becoming a source of regenerative cells. Muscular and nervous cells, after dedifferentiation, appear to be capable only to differentiate in the original cell type; while connective tissue cells (fibrocytes) may originate from fibrocytes or amoebocytes. In the latter case there would be dedifferentiation, cellular division and redifferentiation in another cell type.

These results were compared with Lange's observation and the same stages can be described for the three species (*Sepia officinalis*, *Sepiola atlantica* and *Octopus vulgaris*): wound healing (stage 1); blastemal formation and early growth (stage 2); growth stage (stage 3); differentiation and morphogenesis (stage 4 and 5); functional recovery (stage 6).

Only recently, a new interest on the ability of cephalopod in regenerating appendages was resumed (Rohrbach and Schmidtberg, 2006; Tressler et al., 2014.; Fossati et al., 2015).

Impairment of the function after arm lesion has been reported after arm amputation in cuttlefish (*S. officinalis* and *S. pharaonis*) soon after lesion: swimming, prey manipulation and posturing were affected. However, recovery of the function reappears few days later (Tressler et al., 2014).

These studies provided a detailed description of the morphological changes involved in arm regeneration; the only account we have of the molecular mechanisms involved concerns acetylcholinesterase (ACHE) (Fossati et al., 2015). ACHE is expressed in developing and regenerating arms of octopus. In the former, expression is localized in a cluster of cells likely

forming neuroblast cells; in the latter, it starts to be expressed in undifferentiated cells of the mesenchymal tissue of the tip. In both cases, however, during differentiation of the tissues, its expression is localized to the axial nerve cord, muscles fibers and neuromuscular components of the suckers. This pattern might suggest a role in morphogenesis for ACHE in non-cholinergic processes

The special case of the sexual arm

Interesting results were also obtained on the investigation of the regenerative process of cephalopod sexual arm, the hectocotylus (Steenstrup, 1856; Taki, 1944; O'Dor and Wells, 1978; Bello, 1995). These studies were initiated at the Stazione Zoologica Anton Dohrn by Enrico Sereni, which left open the question of a sex-hormones control on the regeneration of this specialized arm. To answer this question, castration was performed in *Octopus vulgaris* before hectocotylus tip removal in males and corresponding arm in females (Callan, 1940). Complete regeneration of the original structures was observed in both sexes suggesting that the development of a sexual or "normal" arm doesn't depend on hormone secretions of the reproductive system.

Taki 1944 Studies on Octopus. 2. Sex and genital organs of females and males

Further details were provided by O'Dor and Wells (1978) who carried out an experiment on the effect of forced maturation on *O. vulgaris*, through induced gonadotropin release by the optic gland. Arm-cropping was performed on these animals discovering that, in general, precociously maturing females and males regenerate their arms slower than control animals and, more importantly, hectocotylized arms regenerate faster than other arms of the same animal probably due to the importance of this organ for reproduction.

Although able to regenerate even faster than other arms, the sexual arm seems to be less susceptible to injury, compared to other arms (Bello, 1995). Some cephalopod species are indeed known to hold this arm close to the body during foraging likely to protect it (Huffard et al. 2008) due to its importance in mating.

Cornea and lens regeneration

As in vertebrates, cephalopod eye is composed of cornea, lens and iris. However, two main aspects distinguish them from vertebrate eye: cephalopod retina is not inverted and there are no bipolar or ganglion cells (Wells, 1978). They possess polarized sensitivity which might be required for contrast enhancement, target recognition and unmask fish camouflage (Shashar et al., 1996), thus being fundamental for survival.

Only two accounts are available on the ability of cephalopods to survive and recover from lesion of the eyes. A brief appendix is present in Lange 1920, in which a few words are spent on the effect of lens extirpation. Survival of operated animals is greatly affected by the surgery, however she could account for some animals that lived for 10 weeks post-surgery. Soon after injury, these animals lost the ability in perceiving light, which was regained eight weeks later.

Interestingly, cornea regeneration was reported to be extremely rapid in two species of octopus, *Octopus dofleini* and *O.vulgaris* (Dingerkus and Santoro, 1981). In the first species, an 18 kg female, the damage occurred in nature before capture. Upon inspection, it was observed that one cornea was missing, which required 10 days to completely regenerate and become indistinguishable from the contralateral uninjured eye. To further confirm this finding, two female of *O. vulgaris* were injured under cryoanasthesia, removing one cornea per animal. Complete regeneration occurred respectively in 9 and 10 days.

Central Nervous System regeneration

Even though not studied in details, information regarding the ability of cephalopods in regenerating central nervous system has been produced by Young and his co-workers and reported 1971. Young, indeed, run many experiments consisting in the removal of specific brain areas of *O. vulgaris* with the aim of evaluating impairment in learning capabilities after lesion that led him face with this extraordinary capability. He described formation of scar tissue above the cut surface after removal of the vertical lobe, in the supraesophageal mass, identifying some regenerating fibers 34 days after surgery; it was hypothesized that some of these fibers might come from the optic tract, while other seemed to come from deeper (e.g. the celebral tract and from the palliovisceral system). Regenerating nerve fibers were identified also 4 days after removal of the subvertical lobe and 16 to 29 days after bilateral section of the optic tracts. Unfortunately those are the only available accounts regarding this matter.

Brief outline of pallial and stellar nerve regeneration

Dr. Leon Fredericq, during his studies on *Octopus vulgaris* physiology in 1878, discovered and described for the first time the phenotypical effect of cutting one of the two pallial nerves. He observed complete paralysis of respiratory muscles on the side of lesion and paling of the skin due to the effect of denervation of chromatophores. After this first observation, Sereni and Young started a series of phenotypical, morphological and physiological observations on the consequences of the transection of the pallial nerve and the stellar nerves, together with the removal of the entire stellate ganglion. The first reports go back to 1929 (Sereni, 1929; Young, 1929) where fibers degeneration of pallial and stellar nerves and lipid material formation was observed. In addition, clot formation between the two stumps of the pallial nerve was highlighted. No signs of regeneration of the nerve or restoring of function were detected. However, the authors stressed the ability of the skin in coloring again after 3-5 days from denervation, in a manner independent from central nervous system.

These studies, beside being pioneer of the following regenerative investigation, allowed a first interpretation of the connections between CNS and PNS through the pallial nerve.

More than 200 animals of seven different cephalopod species allowed identification of degeneration and regeneration phenomena following pallial and stellar nerves lesion (Young, 1932; Sereni and Young, 1932). Nerve injury induces formation of scar tissue mainly produced by amoebocytes (blood cells) which also infiltrate the stumps. Amoebocytes actively proliferate

amitotically and appear to phagocytose among nerve fibers. Degeneration of axons is mainly observed in the peripheral stump which breaks in lumps, while close to the lesion tip ends swell and later branches. In the central stump, fibers are able to grow either through the scar, toward the peripheral stump, or laterally and backwards. Regeneration and degeneration phenomena are clearly correlated to water temperature, with speed increasing for both at higher temperatures (Sereni and Young, 1932; Young, 1972). 11 to 18 days post lesion, vigorous regeneration of the periphaeral stump is observed. Again Functional regeneration required at least three months.

Sectioning of the pallial nerve doesn't produce any effect on stellate ganglion cells, while if the lesion is performed on stellar nerves, ganglion cells undergo retrograde degeneration. In this occasion, no degeneration of the ventral neuropil is observed, but only of the dorsal one. Degenerating fibers are although visible in the pallial nerve (Young, 1972).

Functional regeneration appears at different timing depending on water temperature and lesion method (crush vs cut). First signs of recovery appear from 30 to 65 days post injury, although majority of the animals require 3 to 4 months for complete regain of function (Sereni and Young, 1932; Young, 1972; Sanders and Young, 1974).

Anatomy of the stellate ganglion and pallial nerve

Octopus vulgaris possesses a pair of pallial nerves, one for each side of the mantle, originating from the posterior part of suboesophageal mass, which is part of the central nervous system (Young, 1971; Budelmann and Young, 1985). Each of the nerves runs inside a "muscular bridge" (Sereni and Young, 1932, p. 177) facing the internal cavity of the mantle. Majority of the fibers of the pallial nerve are directed to the stellate ganglion: here some of them pass without making synapsis to innervate chromatophores, while some others contact motor neurons which then innervate mantle muscle. Each ganglion gives rise to several stellar nerves which contains afferent and efferent fibers connecting muscles and chromatophores in the periphery. Some motor fibers of the pallial nerve do not reach the stellate ganglion as they innervate retractor muscles in the capsule of the liver.

Pallial nerve

Each pallial nerve contains around 16000 fibers (Young, 1965). Even though separation is not sharp, three different components have been identified in the pallial nerve at its origin; these fibers have indeed been separated by size and a putative role has been assumed for them: ***i.*** around 3200 fibers with a diameter of 2-6 µm directed to the stellate ganglion and ~600 between 6-16 µm to the head retractor muscles; ***ii.*** Around 2300 fibers, less than 4 µm in diameter, innervate the chromatophores; ***iii.*** very small sensory fibers (< 1 µm and <2 µm) that could not be counted (Young, 1965; Young, 1971; Budelman and Young, 1985).

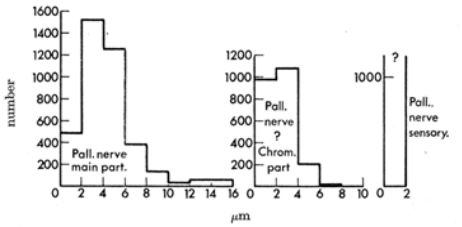

Each nerve fiber in the pallial nerve is enveloped by a tube of connective tissue and no trace of myelin was ever identified (Sereni and Young, 1932). Transverse fibers of connective tissue bound single tubes together and an additional outer connective layer enwraps the whole nerve (Sereni and Young, 1932; Young, 1932; Young, 1972).The connective tissue of the nerve forms a syncytial reticulum with that in the neuropil of the stellate ganglion.

Stellate ganglion

The stellate ganglion contains around 120000 monopolar neurons, distributed on a external cortex which surrounds the central neuropil (Young, 1972; Monsell, 1977). On the horizontal plane the ganglion can be divided in two distinct parts: a ventro-medial composed exclusively of large cells (around 31500 cells with a diameter >15 µm) and a dorsal- lateral containing both large and small cells (around 87800 cells, majority of them with a diameter of <15 um) (Young, 1972). These small

cells are present in the dorsal part of the stellate ganglion, in particular in the inner region of the cell layer, close to the neuropil. They were identified as amacrine cells (microneurons) as similar to the amacrine cells found in the vertical, the subfrontal and the optical lobes. Cobalt and HRP application into the pallial nerve also demonstrated the presence of centripetal cells inside the ganglion, with the axons pointing toward the pallial nerve (Monsell, 1977; Monsell, 1980). They are probably sensory cells, which may serve for transmitting the information from the substellar organs, the latter considered to be stretch receptors.

TABLE 1. CELLS OF THE STELLATE GANGLION

Stellate ganglion of *Octopus*. Numbers and diameters of cells

diam./μm	ventral side	dorsal side
< 5	0	16 600
10	0	36 000
15	8 100	16 400
20	5 000	8 900
25	3 500	5 900
30	5 400	1 600
35	4 800	1 050
40	3 000	450
45	1 200	450
50	300	150
55	100	150
60	100	150
	31 500	87 800

TABLE 2. ALL STELLAR NERVES OF ONE SIDE

diam./μm	ventral roots	dorsal roots
2	2 600	10 280 (really far more)
3	4 240	4 960
4	5 680	4 440
5	6 880	2 720
6	2 520	1 640
7	4 760	440
8	4 040	40
9	520	120
10	280	—
11	40	—
	31 560	24 640 (really far more)

The pallial nerve enters the ventral part of the ganglion, which is the one facing mantle cavity, while 26 to 40 stellar nerves (Young, 1972; Buhler et al., 1975) arise from the dorsal part of the ganglion. Each stellar nerve has two roots, each departing from a part of the ganglion; the two join at the ganglion surface. The ventral root contains only large fibers while the dorsal contains both large and small fibers. Inside the ganglion, abundant glia and the gliovascular tissue are found; the latter is a network of collagen-containing extracellular spaces (Stephens and Young, 1969; Young, 1972) ; Monsell, 1977; Monsell, 1980). Glial cells have ovoid nuclei, with fine processes present both in the neuropil and among cell layer (Monsell, 1977). While glio-vascular channels are not found among amacrine tracts, glial cells are able to penetrate those fibers (Monsell, 1977).

Origin of fibers in the Brain

Majority of the fibers of the pallial nerve take origin from the dorsal and ventral walls of the palliovisceral lobe of the subesophageal mass. Some other, instead, come from the posterior and anterior chromatophore lobes (Young, 1971; Budelmann and Young, 1985). A small number of cells soma has been instead identified in the magnocellular (Budelmann and Young, 1985; Saidel

and Monsell, 1986), visceral, anterior pedal lobes of the subesophageal mass, and from the superior buccal lobe of the subesophageal mass (Saidel and Monsell, 1986).

Into the palliovisceral lobe fibers of the pallial nerve branches to five destinations: ***i.*** fibers to the chromatophore lobes; ***ii.*** Fibers to the palliovisceral lobe; ***iii.*** Fibers to the median basal lobe; ***iv.*** Fibers to the magnocellular lobe; ***v.*** fibers to the brachial lobe. Motoneurons of the anterior and posterior chromatophore lobes send projections both to nerve cord in the arms and to the pallial nerve. Strikingly no afferent fibers were ever detected in these lobes coming from the pallial nerve, thus suggesting that that the control on colour changes comes through the eyes and the lateral basal lobe .

Beside afferent fibers to the magnocellular lobe, also efferent fibers to the pallial nerve where detected from this lobe. They were assumed to be involved in avoidance reaction.

The medial basal lobe receives afferent fibers from pallial and brachial nerves and also from posterior superior ophthalmic and superior antorbital nerves. It may be responsible, through connection with the magnocellular lobe, for the control of avoidance reactions.

The pallial nerve sends afferent fibers to the palliovisceral lobe, probably the afferent axons from receptors in the skin; in addition, cell bodies found in the same lobe, whose fibers run in the pallial nerve, sends efferent to the stellate ganglion probably controlling muscles in the mantle for respiration and locomotion. No direct connection between optic lobes and pallial nerve.

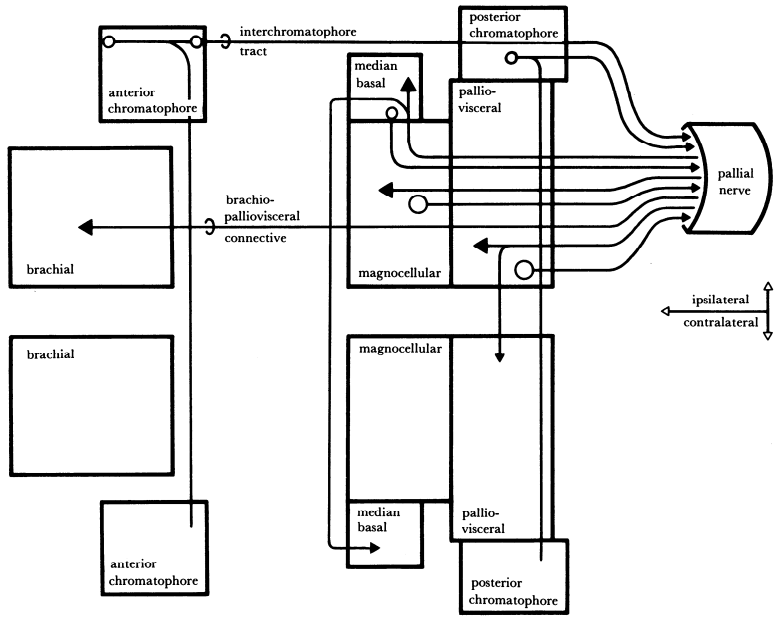

FIGURE 61. Schematic presentation of the afferent and efferent brain pathways of the pallial nerve of *Octopus vulgaris*, as obtained by centripetal cobalt filling. Conventions as for figure 60.

Function

Each pallial nerve, through the stellate ganglion, provides neural network control for breathing and skin patterning on the ipsilateral side of the mantle, innervating three sorts of muscles: ***i***. mantle muscle ***ii.*** skin muscle ***iii.*** chromatophores muscle. For the motor control of breathing is worth to note that the contraction is biphasic: constriction of the mantle is due to contraction of

circular layers of muscles, while active thinning of radial fibers leads to mantle expansion (Monsell, 1977).

Skin pattern is instead mainly obtained through neuromuscular organs distributed in the skin, namely the chromatophores. Those organs present a sacculus containing pigments that can be stretched and retracted through contraction and relaxation of 15-25 radial muscles (Messenger, 2001). Stimulation studies have allowed the outlining of a map of the projection areas of the stellar nerves. It was found that, even if different stimuli can evoke independent response of one of the three types of muscles, the area of projection coincides (Bühler et al., 1975).

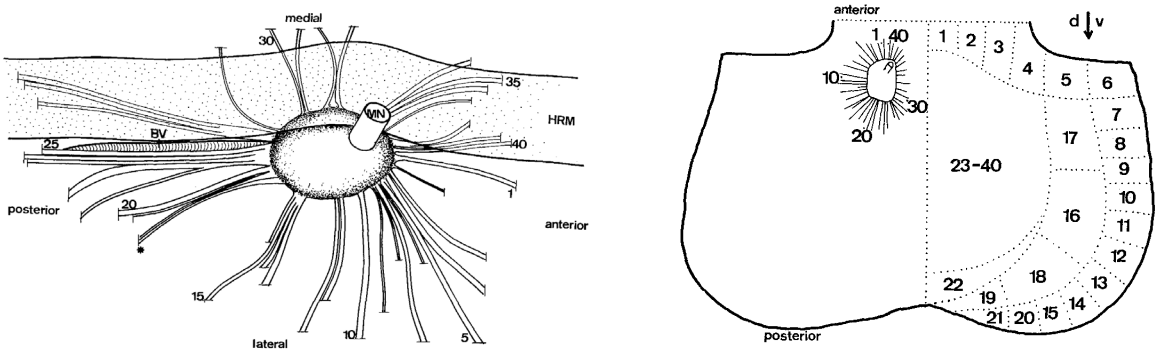

(Bühler et al., 1975)

The transection of a nerve leads to immediate paralysis of respiratory mantle muscle on the denervated side, chromatophore relaxation and consequent paling of the mantle (Fredericq, 1878; Sereni and Young, 1932; Sanders and Young, 1974). The complete regeneration of the pallial nerve and functional recovery require approximately three to four months (Sanders and Young, 1974).

Results

Structural modifications and cellular involvement

Intro

Inflammation, scarring and hemocytes infiltration

Large hemorrhagic areas were observed in the damaged connective tissue and muscle lesioned to expose the pallial nerves of both sides. This was due to the breakage of vessels that run along the pallial nerve (Isgrove, 1909). Scar tissue appeared in all the injured areas, i.e. muscles, connective and nerve tissues, even though the extent of the cicatricial tissue in the sham control appeared minimal relative to the scars formed post lesion (Figs 3, 4).

Two to three days after surgery, a thick scar appeared separating the cut ends of the nerve (Figs 3A, B). The scar impeded the two stumps to come into contact (Fig. 3A). However, this did not represent a permanent barrier for the axons outgrowth as regenerating fibers were later able to grow across it (see following description).

We calculated the size of the scar by counting the number of cells both in the sham control nerve and at the same level in the lesioned nerve. At three days p.l. we found an average of 950 cells per stack (CL), while in the lesioned nerve this number appeared to be about three times higher (LL: 3000 cells per stack; $p = 0.043$ after Student's *t*-test; Fig. 6A). The number of cells forming the scar decreased to around 1800 cells per stack (LL) a week after injury (7 days p.l.) in the lesioned area, a number that appeared to be still different from the cells counted in control areas (CL: 1100 cells; $p < 0.001$ after Student's *t*-test). Finally, a significant increase of the number of cells in respect to the controlateral area was observed in the peripheral side of the lesion (14 days p.l.; L_P1 and L_P2: 1900 and 2000 cells respectively; C_P1 and C_P2: 950 cells; L_P1 vs C_P1, $p < 0.001$; L_P2 vs C_P2, $p = 0.019$ after Student's *t*-test; Fig. 6A). Fourteen days post lesion a large reduction of the size of the scar was observed.

The contribution of hemocytes to scar resulted not quantifiable under our experimental conditions. However, these appear to be the larger component. In fact, several cells identified by morphology as hemocytes contributed to scar formation at the lesion site (LL) and infiltrated between regenerating fibers of the central stump (Figs 3B,E).

Numerous hemocytes also infiltrate the peripheral stump in contact with regenerating fibers at 14 days p.l.; these were not evident at earlier time-points in this area. The main source of hemocytes inside the nerve appeared to be the blood vessel running inside the pallial nerve, which was also transected during surgery (Fig. 3B). This is consistent with observation made by Sereni and Young

(1932), who observed “amoebocytes” (i.e. hemocytes) contribute to the scar and infiltrate the stumps.

Within the scar hemocytes appeared to undergo structural changes from the classical spherical form they retained in the vessels, to a spindle shape when they reached the site of lesion. This observation is compatible with those reported by Féral (1988) during arm regeneration in the cuttlefish (*Sepia officinalis*) in which hemocytes (i.e. blood cells) migrated to the wound to form the blastema.

Cryostat sections of the sham and lesioned pallial nerve were also analyzed through label-free two-photon microscopy, in collaboration with Prof. Dr. Matthias Kirsch at the Klinik und Poliklinik für Neurochirurgie in Dresden. Label-free two-photon microscopy is extremely helpful in *ex vivo* and *in vivo* study in the identification of structures and molecules and in the evaluation of disease states in mammals. Multimodal nonlinear optical microscopy has proven indeed to be a powerful tool for the detection and evaluation of many pathologies such as Alzheimer’s disease, cancer, myelin pathologies, multiple sclerosis, and more (Zipfel et al, 2003; Le et al. 2007; Imitola et al. 2011; Schain et al., 2014) whose diagnosis and progression is usually difficult in vivo, especially for pathologies involving CNS. This methodology has also been applied for the study of axon injury after spinal cord contusion or lesion (Galli et al., 2012; Lorenzana et al., 2015; Uckermann et al., 2015). Anti-Stokes Raman scattering (CARS) allows visualization of lipid content, endogenous two-photon excited fluorescence (TPEF) is used for endogenous fluorescent molecules and second harmonic generation (SHG) mainly for collagen, thus giving a great deal of information on axons degeneration and regeneration, extracellular matrix composition, microglia/macrophages distribution. Analysis of the CARS and TPEF, tested for the first time on octopus samples, allowed clear visualization of hemocytes and blood inside the hemorrhagic areas, confirming also the presence of a blood vessel inside the pallial nerve. The contribution of hemocytes to the formation of the cicatricial tissue, their infiltration inside the lesioned areas and in the nerve stumps was also evidenced. TPEF highlighted an additional signal inside the blood vessels, which is not ascribable to blood.

Degeneration* vs *axonal regrowth

Regeneration occurred differently between the central and peripheral nerve stumps. The central stump was characterized by intensive axon growth already three days after surgery. On the other

hand, the peripheral stump of the nerve towards the stellate ganglion showed mainly degenerative processes.

The main axonal re-growth was observed in the proximal area of the central stump (Figs 3A, B; areas corresponding to L_C2 in Fig. 1) with fibers oriented in many different directions, opening in a fan-like shape, revealing a disorganized pattern. The majority of the regenerating nervous fibers led toward the scar tissue, though some of them penetrated the scar. Five to seven days post lesion the regenerating fibers at the level of the central stump continued growing in multiple directions, but most of them were observed to move past the cicatricial tissue, contacting the peripheral axons (Figs 3E, 3F) and starting to assume a spike-like structure. Axon breakage in the peripheral stump involved a larger area than the previous stage (Fig. 3G). Multiple lumps formed by debris of degenerating axons appeared to be swollen. Neurofilaments (detected by NF200 antibody) appeared to accumulate towards these swollen neuronal terminal endings.

Backfill experiments and label-free two photon microscopy confirmed the data obtained with IHC, integrating new details. The neural tracer (i.e. neurobiotin) was seen to fill the fibers of the central stump: far from the lesion site the nerve retains its normal appearance, but close to the original site of injury, they fibers started to regenerate more disorganized in the center, but starting to shape all in all in a spike-like structure. No signal was detected in the peripheral stump, nor in the ganglion.

In intact samples, CARS allowed the visualization of the axons of the pallial nerve, together with neurons and neuropil of the stellate ganglion. Inside the lesioned nerve instead, axons were again visualized in both stumps, however the degenerating fibers of the peripheral stump were highlighted with a stronger signal. They were indeed perfectly recognizable and distinguishable from intact or regenerating fibers. Due to the fact that CARS recognizes mainly lipids, the stronger signal might be explained by lipoid materials released by degenerating axons, which was also hypothesized by Young (1929).

TPEF, instead, showed the cytoplasm of the neurons inside the stellate ganglion, but no axon could be detected. This is likely to be fluorescence emitted by the metabolic waste product lipofuscin, which is known to accumulate in cephalopod nervous tissues (Semmens et al., 2014). Additionally, a strong signal is detected in the degenerating fibers of the peripheral stump and in the regenerating fibers of the central stump. Signal appeared so clear that also the few regenerating

633 fibers of the peripheral stump and the little degeneration of the central stump were easily
634 recognized. These signals were hardly detectable with IHC and histology staining.
635 Significant changes in the nerve regeneration process were observed two weeks after the injury.
636 At this time point, we observed a retraction of at least one of the two stumps, probably consistent
637 with degeneration of the peripheral stump. This produced an apparent increased distance
638 between the two stumps, compared to the first time-points investigated.
639 We observed numerous fibers directed toward the peripheral stump appearing well organized and
640 forming a defined spike-like structure (Fig. 3H). Nevertheless, the neural fibers in the central
641 stump, although remaining confined into the external connective layer, still generally showed a
642 disorganized appearance inside the spike. In the opposite stump, even though degeneration
643 appeared more intense, many regenerating fibers protruded for several microns within the debris.
644 (Fig. 3I). In all cases the two stumps were directed toward each other and made contact.
645 Regeneration of the central stump and degeneration of the peripheral stump has also been
646 previously detected in the pallial nerve. Sereni and Young (1932) described the ability of fibers in
647 the central stump to grow either through the scar, toward the peripheral stump, or laterally and
648 backwards, without a well-defined direction. Breaking axons produces large spheres which are
649 probably invaded by amoebocytes and that last even after functional regeneration occurs. 11 to
650 18 days post lesion, vigorous regeneration is observed from the pallial nerve, which is probably
651 afferent fibers from periphery (Young, 1972).
652 Regeneration/degeneration phenomena observed at the different time-points were also identified
653 by considering the area occupied by the neuronal filaments. The major changes where observed in
654 the lesioned nerve at the level of the central stump (L_C2) seven days post lesion (L_C2 vs C_C2
655 neurofilament area, $p < 0.001$ after Student's *t*-test; Fig. 6B) due to axonal regrowth in the central
656 stump (Figs 3A, D). Degeneration resulted in considerable axonal loss when compared with
657 controlateral nerve (see Fig. 4), revealing a reduced neurofilament area (L_P2 vs C_P2, 3 and 7 days
658 p.l., $p < 0.010$ after Student's *t*-test; Fig. 6B).
659 Fourteen days after lesion a similar situation was found in the lesioned nerve at the level of the
660 peripheral (L_P2) stump (neurofilament area, lesioned vs controlateral side, $p = 0.001$ after
661 Student's *t*-test), but not when the central stump was considered (L_C2 vs C_C2, $p = 0.924$, NS after
662 Student's *t*-test). In the sham controls a constant number of fibers were detected at both sides
663 (i.e. central vs periphery) and corresponding locations (Fig. 6B).

Backfill experiment allowed identification of the pathway followed by axons for target re-innervation. Indeed, even though in the original site of lesion axons retained a disorganized appearance distributing in several directions, majority of the fibers of the central stump were seen to enter the peripheral stump and from there to penetrate the stellate ganglion. Inside the ganglion, these fibers distributed as a net among motor neurons. Axons were also able to leave the ganglion through the stellar nerves, to reach their final target: chromatophores and skin muscles. No positive cells were ever found inside the ganglion.

Connective tissue

Trichrome staining, backfill and label-free multiphoton experiments pointed out the leading role of the connective tissue during the regenerative process.

A few days after surgery, namely two-three days p.l., the internal connective layers in the central stump tied around the cut axons. The original site of transection was indeed recognizable due to the fact that this tissue did not regenerated together with axons, but instead contracted on site. Regenerating axons were however able to grow beyond it growing in different directions, as described previously. Internal layers of connective tissues re-appeared around re-growing fibers of the central stump only two weeks after lesion.

In the opposite stump, instead, the internal connective tissue didn't undergo evident structural changes, remaining intact around degenerating axons, even though some nuclei showed a distorted shape few days after injury, as also observed by Sereni and Young (1932).

The external layer of connective tightened around both stumps to seal the cut ends of the nerve; narrowing started to result evident around five to seven days post lesion even though a spike-shaped structure of the central stump appeared only in the second week post lesion. In the meanwhile regenerating fibers appeared also in the peripheral stump; those fibers, not visible at earlier time points, appeared well-organized in fascicles enveloped by connective tissue directed toward the opposite stump.

The most interesting evidence of the leading role of the connective tissue came from SHG signal, detected trough label-free multiphoton microscopy. It enabled to distinguish the connective tissue from the surrounding structures, especially axons, and highlighted the internal connective tissue layers, i.e. those separating the pallial nerve into fascicles, and the external layer, which envelops the whole nerve. SHG detection combined with backfill experiments on whole mount nerves confirmed the plasticity of this tissue in reorganizing and narrowing around both stumps and in shaping a spike-like structure in the central stump. The connective tissue appeared to create a

scaffold between the two stumps on the ventral side, shaping and bridging them toward each other.

Gene expression changes during regeneration

A short overview on gene of interest

An extremely complex biological machinery has been highlighted during regeneration studies in several species. A great number of genes and pathways have been identified as involved in the regulation of repair phenomena determining its success or bringing to its failure. Many of these pathways are shared among higher vertebrates and extremely simple invertebrates, while other genes appear to be specific for particular species. The so called regeneration-associated genes (RAGs) comprise structural proteins, pro-axon growth signaling proteins, transcription factors and neurotrophic peptides. New findings suggest the possibility that activation of these genes upon injury might be regulated by epigenetic mechanisms, which modulate access to chromatin for transcription.

Our aim was to identify RAGs and genes involved in epigenetic modifications for the first time in cephalopods and evaluate their putative involvement in the regeneration phenomena of the pallial nerve. Based on the available literature on gene expression profile during nerve regeneration, we selected a list of putative involved genes. Based on the data of the RNAseq by Petrosino et al. we were able to identify a set of 29 genes (see Table) in the octopus transcriptome.

Histone lysine methyltransferases (HKMTs) and lysine (K) demethylases (KDMs) were identified.

PCR1

PCR2

….

Musashi

….

….

Gene expression changes

….

Localization of proteins in the stellate ganglion and pallial nerve

Seven days following injury, semiquantitative PCR showed a change in gene expression. In particular two genes out of 29 resulted to be up-regulated in the cut nerve compared to the sham control nerve: MAPK and Musashi (Msi).

Through IHC, we tested the expression of phospho-p44/42 MAPK (ERK-P) and Msi. They both resulted to be expressed in the connective tissue of the transected nerve. ERK-P is a mitogen-activated protein kinase involved in many cellular programs (proliferation, differentiation, cell death), while Msi is a RNA binding protein, important for maintenance of the stem-cell state. Both proteins are highly conserved across the animal kingdom (from Planaria to human) and appeared to be involved also in octopus nerve regeneration.

Localization of ERK-P

In the uninjured nerve, ERK-P appears to be expressed at extremely low level, hardly detectable through IHC. Its expression inside the neuropil of the stellate ganglion and in some of its neurons appeared instead constitutively present. Following injury, the levels of ERK-P highly increased in the cytoplasm of connective tissue cells of the lesioned nerve, compared to the control. Indeed, immunoreactivity of ERK was extremely low, even though detectable in both, sham control nerves and uninjured nerves at all time-points investigated (2, 3 7 and 14 days post lesion). The lesioned nerve instead, showed high levels of expression of the phosphorylated protein.

Specificity of the commercial antibody developed against human p44 MAP kinase was tested through western blotting on octopus supraesophageal mass. The protein showed to be highly specific, as only one band was found, corresponding to 42 kDa.

The protein resulted to be highly expressed at 2, 3 and 7 days after lesion, while two weeks post-surgery the protein returned to basal level of expression. The lesioned area (LL) appeared to be the one presenting the highest levels of expression, together with the proximal areas of both stumps (L_C2 and L_P2). The intensity of the signal decreased in the distal areas (L_C1 and L_P1) however being anyway higher than in the control nerves.

The ERK-P signal appeared very intense in regenerated fibers, while absent in the degenerated one. The big lumps formed by breaking axons were indeed strongly marked with NF, as previously stated, but ERK-P signal was slightly detected.

Localization of Msi

Msi mRNA resulted to be highly expressed in pre-hatchling, hatchling and post-hatchling samples. Interestingly, in arm tip it showed to be more expressed than in whole arm, while arm muscles showed almost no expression. The stellate ganglion, also appear to express Msi mRNA.

As these preliminary results suggested an involvement of Msi in octopus development, we decided to test the hypothesis that it could also be involved in nerve regeneration. Its expression was tested through IHC, western blotting and PCR. The commercial antibody against human Msi didn't give any evident positive signal in uninjured control nerves, while a slight positivity was detected in the sham nerve. In the lesioned pallial nerve, instead, Msi protein showed to be highly expressed in the nuclei of connective tissue cell, both the one singly enveloping axons, that . Positive nuclei were identified at seven and 14 days p.l., while they could not be detected at two or three days p.l. The signal appeared as dotted and condensed in specific points of the cell nucleus.

Seven days post lesion signal could be detected in the nuclei of internal and external connective tissue layers nuclei in the lesion area (LL) but also in proximal and distal areas of both stumps. Not all cells resulted to be positive for Msi, but a distinction could not be made on the typology of cells expressing the protein.

Two weeks p.l., positive cells were again identified in the nerve; however, this time, positive cells appeared to be restricted to LL and LC2 areas in the central stump. Only a few cells appeared to be positive in the peripheral stump.

PCR analysis further confirmed these data. Semi quantitative PCR demonstrated that uninjured pallial nerve basally expressed Msi, even though at extremely low level. Seven days post lesion an intense increase of Msi mRNA was detected in both the lesioned and sham control pallial nerve, even though in the former gene expression is doubled compared to the latter.

Inside the stellate ganglion, no differences in Msi expression were detected between the control and the lesioned side, at least at

seven days p.l. No difference could also be detected through IHC, which showed Msi signal inside ganglion neurons. Glial cells inside the neuropil of the ganglion never appeared to be positive to Msi.

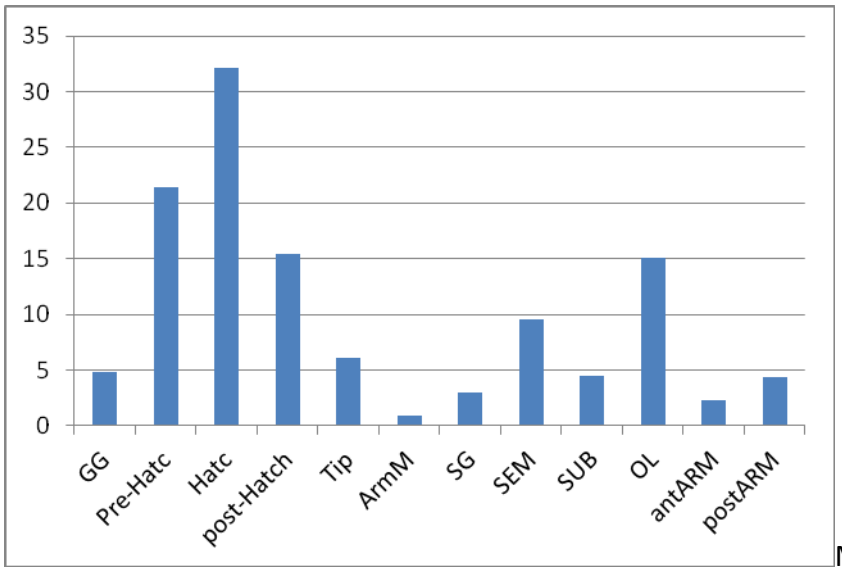

785 Msi expression

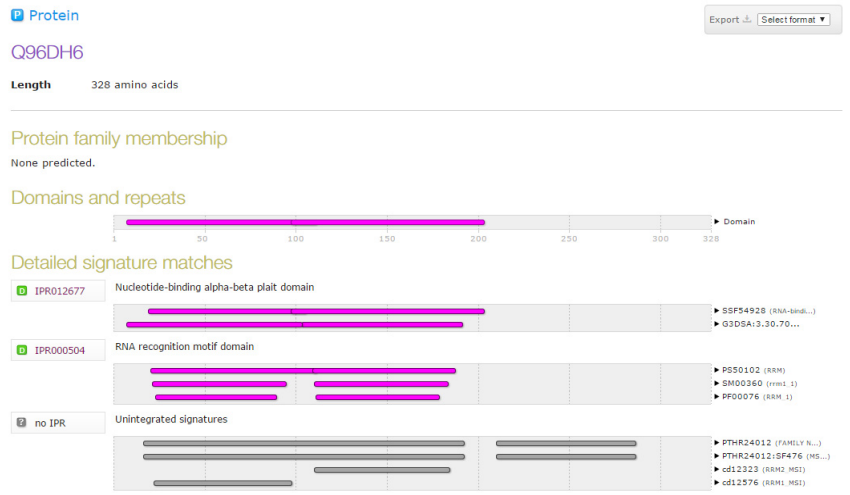

786

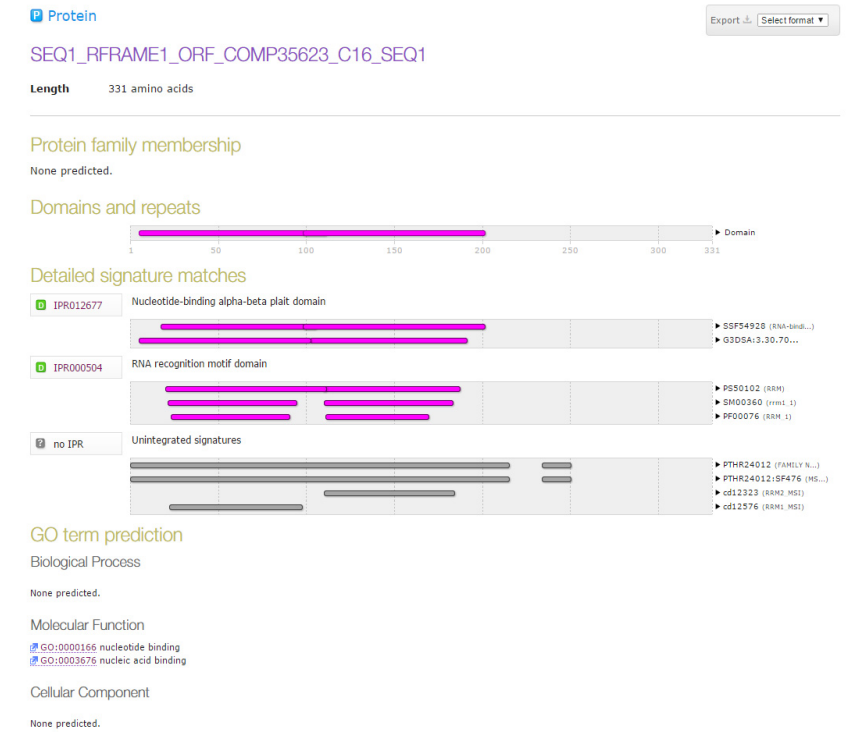

787

788 ***Localization of epigenetic modification***

789

790 ***Cell proliferation***

791 Large numbers of hemocytes were observed three days post injury contributing to the formation
792 of the scar tissue between the two stumps. They also provided the main source of proliferating
793 cells found at this time-point (Figs 5A-E). We counted 20 PHH3 positive cells (from a total of 3000
794 per stack) at the lesioned site (LL, Fig. 6C; Number of PHH3 cells at LL vs CL: p = 0.008 after

795 Student's *t*-test). Mitotic hemocytes were also found within the blood vessel running into the
796 central stump, leading to the injury and at the level of the connective tissue surrounding the nerve
797 (Fig. 5B; number of PHH3 cells at L_c2 vs C_C2: $p < 0.001$ after Student's *t*-test). The sham control
798 showed some proliferating cells in the external connective layer, but no proliferating hemocytes
799 were detected inside the nerve or in the inner blood vessels (Figs 4, 6C).
800 Seven days after injury the number of proliferating cells remained similar (PHH3 *vs* total cells: 25,
801 1900 cells per stack, LL vs CL: $p = 0.001$ after Student's *t*-test) to the number observed during the
802 previous time-point. PHH3 positive cells did not appear restricted to the lesioned site, but rather
803 were expanding towards new growing fibers (L_C2, PHH3 vs total cells per stack: 46, 1500
804 respectively; L_c2 vs C_C2, $p = 0.001$ after Student's *t*-test; Figs 5F, 6C). At the same time-point we
805 also observed other proliferating cells with morphological features typical of the connective tissue.
806 These were characterized by larger elongated nuclei and were positioned within the tissue around
807 nerve fibers (Fig. 5I).
808 Similar cells occasionally appeared in the sham control nerves and in uninjured nerve (data not
809 shown), suggesting a basal level of proliferation of the connective tissue. However, these numbers
810 were low compared to the injured nerve. We found on average zero to three proliferating cells per
811 stack in the sham nerve (Fig. 4), and between zero and one in the uninjured nerve.
812 A large number of proliferating cells were found inside the lesion site 14 days after injury (PHH3 *vs*
813 total cells: 25, 1800 cells per stack; LL vs CL $p < 0.001$ after Student's *t*-test). A similar number was
814 also detected in the peripheral stump (PHH3 positive *vs* total cells per stack, L_P2: 28, 2000; L_P1: 6,
815 1900; $p = 0.009$ after Student's *t*-test; Figs 5K, 6C). The great majority of these cells were identified
816 as connective tissue-like cells and hemocytes.
817 Finally, we detected proliferating cells at the level of the peripheral stump. These were also
818 positively marked with the neuronal marker NF200. These cells appeared to be scattered between
819 both degenerating and regenerating fibers (Figs 5L, 5M).
820 Some mitotic cells appearing within the external connective layer were also positive for NF200.
821 The latter were identified at all the time-points in both the injured nerve (Figs 5H, 5J) and the
822 sham control.
823 In any case, no NF200-positive cells were ever found inside the control nerve.
824 Dividing cells were also observed by Sereni and Young (1932) in the lesioned pallial nerve. They
825 were identified as amoebocytes actively proliferating, though amitotically.

826 The antibody PHH3 used in our experiments specifically recognize phosphorylation of H3, at serine
827 28, which in mammals coincides with the induction of mitotic chromosome condensation, thus
828 suggesting that mitosis instead of amitosis is involved. Involvement and proliferation of connective
829 tissue cells had never been described before.
830
831 ***Target re-innervation and recovery of function***
832 All animals behaved normally and did not exhibit any sign of distress or suffering after surgery
833 (*sensu* Andrews et al., 2013; see also: Fiorito et al., 2014; 2015) and during the following 14 days
834 post-lesion (p.l.). Octopuses attacked their prey promptly in less than 30 seconds in all occasions
835 exhibiting their normal predatory behavior (Maldonado, 1963; Hochner et al., 2006; Amodio et al.,
836 2014) and fed regularly.
837 A full attack response (Packard, 1963; see also Borrelli et al., 2006) was observed as response to
838 the presentation of a crab as natural prey (Maldonado, 1963; Amodio et al., 2014). The effects of
839 the damage due to the lesion appeared mostly on the mantle, ipsilateral to the lesioned side, as
840 deficits in the full expression of body patterns exhibited by the animal.
841 After surgery, the lesioned side appeared pale (Fredericq, 1878; see for definition Borrelli et al.,
842 2006) and no control of chromatic and textural pattern resulted evident (Figs 1C, 2C) and the
843 animals lost the ability in controlling skin papillae. The contralateral side retained the ability to
844 perform the full range of body patterns as in a normal behaving animal (Packard, 1963; Packard
845 and Sanders, 1969; Packard and Sanders, 1971; Packard and Hochberg, 1977; see also Borrelli et
846 al., 2006). A few hours after recovery from anesthesia some animals showed self-grooming actions
847 (Mather, 1998) consisting in arm bending over the head and the mantle surface (Borrelli et al.,
848 2006); grooming was exhibited in proximities of the denervated area and inside the mantle cavity.
849 One to two days later, light brown spots appeared on a white-greyish/pale background while three
850 to five days post lesion the whole dorsal area of the denervated skin had a uniform colored
851 appearance (Fig. 2D). Smooth skin texture was always observed in this phase.
852 In our experimental conditions from seven days p.l. the animals exhibited at rest a marked ability
853 to match the chromatic pattern of the uninjured side (Figs 2E, F). Normal chromatic patterning
854 was not observed on the mantle while the octopus performed an attack response; in these
855 occasions the lesioned side became again pale. No improvement was observed after two weeks
856 post lesion. Indeed, one to two months after injury the control of color and pattern of the skin was

recovered in all animals. In addition, all the animals recovered the ability of controlling papillae formation around one month after lesion.

Nerve lesion also determined impairment of the mantle contractions during normal breathing on the denervated side, with mantle muscle activity appearing jerky and unsynchronized. To evaluate the recovery of the function, we measured weekly the range in length of the opening of the mantle cavity on both sides. Seven days post lesion, mantle contractions was visible impaired and we did not notice a great improvement during the second week, despite the fact that muscular tone increased with time. An impressive improvement was obtained around the third and fourth week post lesion; breathing was finally restored between 30 and 37 days.

In all previous studies 60 to 150 days were required for complete recovery of color function that, in some cases, never occurred (Sereni and Young, 1932; Sanders and Young, 1974) In particular, crushing of the nerve required 8 – 10 weeks for the complete recovery of producing patterns. No animals showed signs of color pattern recover until 50 days post-surgery, nor in summer nor in autumn, six out of ten animals recovered full color pattern (majority between 60 and 69 days), while only for two out of ten it was possible to prove papillae functional recovery (between 30 and 50 days).

When the nerve was cut, four animals over 10 recovered color pattern; although some signs of recovery where visible at 30 days, complete regain of function required 109 d. Seven animals out of 10 recovered the ability in raising papillae.

Macroscopical observations during anaesthesia

At sacrifice, after immersion in the anesthetic solution, the denerved side of the mantle appeared yellowish, while contralateral side and the rest of the body appeared pale as usual classic reaction to immersion in the $MgCl_2$ solution. Only when the dorsal part of the mantle was taken out from the solution, with the rest of the body immersed, dark waves appearing apparently uncontrolled on a white-grayish background were observed on the denerved skin. These waves have been observed by Packard (1992) and referred as “wandering clouds”. They have been considered as due to hyper-excitability of the radial muscles of chromatophores (Sereni, 1930; Sereni and Young, 1932; Sanders and Young, 1974) and appear not to be under the control of the central nervous centers (Sereni, 1929). In addition, in the same conditions the denervated skin resulted to be very

susceptible to mechanical stimuli contracting intensely, compared to the contralateral side which did not respond to stimulation.

The denerved skin also proved to be extremely reactive to touch while the opposite side of the mantle remained pale and insensitive to touch.

The described behavior of the skin at anaesthesia was observed at all time-points from two to 14 days p.l. (namely two, three, seven and 14 d pl.) while when animals were sacrificed after 30 days p.l. or later the denerved side appeared pale as contralateral side, wandering clouds were no longer observed and skin reaction to pinch was absent.

Gene expression

As gene expression changes in cephalopods were never evaluated during regenerative phenomena, a set of 29 genes was found in the transcriptome

Material, methods and approches

Animals

Adult *Octopus vulgaris*, both sexes (body weight: 250-350) caught from the Bay of Naples were kept under standardized conditions (Fiorito et al., 1990; Amodio et al., 2014) in the laboratory. Experiments were conducted during spring of the 2013 (sea water temperature range: 18-22 °C). All the animals were fed with crabs once a day. Octopuses for this study were selected for the absence of any regenerating sign or any kind of lesion, and appearing exploratory driven and healthy (sensu Maldonado, 1963; Hochner et al., 2006). Experiments with live octopuses were carried out before transposition of Directive 2010/63/EU in Italy. Although no authorization was required, all procedures were performed in order to minimize the pain and distress of the animals involved (Andrews et al., 2013; Smith et al., 2013; Fiorito et al., 2014; 2015).

Nerve transection

O. vulgaris were anesthetized by immersion in 3.5% $MgCl_2$ in sea water for 15 minutes, which produced complete relaxation and immobility of the animals (Grimaldi et al., 2007). Anesthetized animals were placed on a surgery table, positioned on a dissecting tray containing the anaesthetic solution. Octopuses were turned on their ventral side, the mantle slightly overturned to expose the nerve and the stellate ganglion nearby; a scalpel was used to make an incision on the internal side of the mantle cutting the skin, muscle and connective tissue enwrapping the pallial nerves. In this way both nerves (left and right side of the animal) were exposed using a skin hooklet. To standardize the site of the injury along the nerve, the diameter of stellate ganglion was measured for each animal, and the same length computed as distance along the nerve to set the site of severing. Left-side nerve remained intact and gently positioned back on its natural position thus serving as a sham control. The right-side pallial nerve was hold with the hook and completely transected using fine scissors. The entire operation lasted less than five minutes.

The completeness of the transection was verified by visual inspection under a stereo microscope. Uninjured samples belonging to other three animals were also collected to assess the effect of lesion on tissues surrounding the nerve.

Following surgery the animals were returned to their tanks and allowed to recover (Grimaldi et al., 2007; Pagano et al., 2011). Full recovery was based observing re-acquisition of the normal posture,

regular breathing rate and return to den; this usually requires less than 30 minutes, and a full predatory response was recorded 60 minutes later (Agnisola et al., 1996; Andrews et al., 2013).

Behavioral observations and animals care

After recovery, octopuses were maintained in experimental tanks and fed on live crab (*Carcinus maenas*) every day following procedures described in Amodio et al. (2014). Predatory responses were videorecorded by remote controlled digital video cameras (Panasonic HDC-SD80), which were hidden from each animal's view. Each presentation lasted a maximum of two minutes (ceiling latency to attack: 121 s) and a failure to attack within this period was classified as "no attack" (Maldonado, 1963; Fiorito et al., 1990; Amodio et al., 2014). Behavioral observations were carried out at the same time of the day, in the afternoon. Video recordings of operated animals were examined to analyze behavior and to detect changes in octopus appearance between the lesioned and the control sides. In particular, chromatic and textural patterns were noted daily during the attack behavior and at rest, for at least 10 minutes before and after the prey presentation in the octopus tank. From video-recordings, two independent observers deduced ***i.*** the latency to attack the prey; ***ii.*** the body pattering and the approximate areas of blanching of the skin (mantle and any other body part) according to the descriptions provided by other authors (Sanders and Young, 1974; Packard, 1991; Packard, 1995b). Body patterning observed during the analysis of video-recordings was coded following Borrelli et al. (2006). Behavioral observations also served as assessment of health and welfare of animals according to principles stated in Directive 2010/63/EU; Signs based on appearance, behavior and physiology were searched from a checklist as part of health monitoring program and eventually recorded (Fiorito et al., 2015).

Collection of samples and humane-killing of octopuses

Animals were humanely killed at three different time-points: three, seven and 14 days after injury. At the selected time-points the octopuses were deeply anesthesized (> 30min) by immersion in a 3.5% solution of magnesium chloride hexahydrate in seawater; death was confirmed by transection of dorsal aorta (Grimaldi et al., 2007; Fiorito et al., 2015).

On the surgery pad, a clamp was used to pinch and hold the pallial nerve during harvesting. Both pallial nerves (cut and sham or control) were collected together with the stellate ganglion and surrounding tissues.

Frozen and paraffin sections

Samples were fixed in paraformaldehyde (4% PFA in sea water; for 1h 30 min), washed in PBS (pH 7.4) and rinsed over night at 4°C. They were cryoprotected in sucrose (30% in PBS; pH 7.4) until tissue sinking, and frozen using tissue freezing and blocking medium (OCT; Leica Biosystems). Longitudinal 30 µm thick slices were obtained using a cryostat (Leica CM3050 S). For paraffin sections, samples were dehydrated through an ascending series of alcohol, cleared in xylene, immersed in paraffin and then cut into 5 µm thick sections.

Immunohistochemistry and histology

Cryostat sections were used for immunohistochemistry. They were air dried for 1h, washed in PBS and Normal Goat Serum (NGS) 5% in PBT (PBS + Tween 0.1%) was used as a blocking agent. Slices were then incubated with primary antibodies, diluted in NGS 1% in PBT overnight at 4°C. Anti-Neurofilament 200 Sigma N5389 (NF-200, 1:2000), and anti-Phospho-Histone H3 Sigma H9908 (PHH3; 1:600) to label axons and detect cell proliferation, respectively were utilized. Sections were then washed with PBT and then incubated with secondary antibodies (1:250; respectively Alexa Fluor goat anti-mouse IgG1 594, and Alexa Fluor goat anti-rat IgG (H+L) 488) for 1h at room temperature. The omission of each primary antibody was used as negative control for each immunostaining. Following washing in PBT, DAPI (diluted 1:1000 in PBS) was used to counterstain nuclei. Paraffin sections were stained for Masson's trichrome (Bancroft and Stevens, 1982) after paraffin removal and rehydration in an ethanol series.

Confocal imaging

Sections labelled with fluorescent dyes were imaged on a Zeiss LSM 710 laser scanning confocal microscope using a 20× air objective. Z-stacks of five areas of the damaged nerve were taken.

The analysis of the events occurring after surgery focused on five areas for each pallial nerve (Fig. 1): the site of lesion (LL), a distal and a proximal area in the central stump (respectively identified as L_C1 and L_C2), and in the peripheral stump (L_P1 and L_P2) of the transected nerve. Analogous areas were identified in the control nerve preparation: corresponding lesion site (CS), a distal and a proximal area in the central 'stump' (C_C1, C_C2), and at the level of the peripheral 'stump' (C_P1, and C_P2).

Morphology and anatomical description

We follow morphological and event descriptions as provided by Young and coworkers (Sereni and Young, 1932; Young, 1971; Young, 1972; Budelmann and Young, 1985). The two stumps have been identified as belonging to central and peripheral sides of the pallial nerve, respectively. According to modern literature on nerve regeneration, these should be named respectively proximal and distal, but here we refer to the classic terminology.

Image and Data analysis

Images were processed with IMARIS 64 7.5 (Bitplane Inc.) for nuclear and mitotic cells counting and neurofilament area calculation. Graphics were generated using the SPSS version 14.0 software (SPSS Inc). One-way or Two-way ANOVAs followed by Bonferroni multiple comparisons test were used whenever indicated. Differences were considered significant at $p < 0.05$.

Backfill protocol

Pallial nerve and stellate ganglion were harvested from control and lesioned animals. All excess tissues around the nerve and ganglion were carefully removed. A Vaseline pool was built in a petri dish with a sylgard bottom.

The bottom of the pool was made using a syringe filled with Vaseline. The far end of the pallial nerve was placed on the Vaseline; following, the pool was built around this nerve ending, leaving the remaining nerve and ganglion outside the pool blocked with a thin pin.

The pool was filled with distilled water and checked for the presence of spills for at least five minutes. Distilled water also favours tracer diffusion. Water was then replaced with tracer solution (Neurobiotin 5% in distilled water) and the pool was closes on the top with other Vaseline. The petri dish is filled with filtered sea water and closed with a lid and sealed with Parafilm. The tracer is left to diffuse for 2 days at 4°C.

After dye diffusion, sea water was drained and Vaseline pool was removed (paying attention that no dye leaks into the bath). The tissue is fixed in 4% PFA in sea water for 2 h at room temperature (RT), on shaker.

Washes in 0,1 M PBS served to remove PFA. Dehydration was performed with ascending ethanol series (30%, 50%, 70%, 90%, 100%) 20 min each. Two changes of methyl salicylate of five minutes each were performed.

Rehydration was then obtained with descending ethanol series (100%, 90%, 70%, 50%, 30%) 20 min each.

The samples were washed with 0,1 M PBS at 37° C, on shaker, for 20 minutes, followed by enzymatic treatment with collagenase/dispase and hyaluronidase in 0,1 M PBS for 30 min at 37° C on shaker. The final concentration of the enzymes is 1mg/ml).

Two washes with 0.1 M PBS and four washes in 0.1 M PBS + 1% Triton X-100 (Tx) followed (15 minutes each).

Samples were placed for pre-incubation in 10% NGS in 0.1 M PBS + 1% Tx overnight at 4° C and the following day incubated with streptavidin Cy3 conjugated (1:200) in 0,1 M PBS + 1% Tx + 10% NGS overnight at 4°C. From this time on, preparations were always kept in the dark.

Samples were washed in 0.1 M PBS and dehydrated with ascending ethanol series (20 min each).

For clearing samples were immersed in 100% ethanol and methyl salicylate 1:1 for 20 min, and then in pure methyl salicylate until the preparation was fully transparent and clear.

For visualization at the microscope, the whole nerve and ganglion were embedded in methyl salicylate in a metal slide (2 or 3 mm thick) closed on both sides by cover slips, closed at the edges with nail polish.

Introduction

Cephalopod molluscs are known for the richness and plasticity of their behavioral repertoire and underlying neural control [1-4]. These animals possess the remarkable ability to heal and regenerate a variety of different tissues [5-7]. Recent work on cuttlefish [8,9], squid [10,11] and octopus [12,13] resumed interest towards this aspect of cephalopods biology, providing new information available. Despite recent experimental studies, detailed knowledge about mechanisms occurring during the different phases of regeneration in cephalopods is still missing.

The common octopus, *Octopus vulgaris,* is known to heal and regenerate appendices, cornea, peripheral nerves and neural pathways within the central nervous systems [5,14-18]. After their original observations Sereni [19] and Young [20] were the first to provide a description of the histological and physiological phenomena occurring in octopus after severing one of the two mantle connectives, i.e. the pallial nerve [18]. Although several cephalopod species were studied in this work, most of the accounts were based upon observations carried out on octopuses (*O. vulgaris* and *Eledone moschata*). A functional recovery was observed only in six cases over 200 lesioned animals, with the earliest signs of functional regeneration seen 65 days post operation [18]. In a series of successive works a better description of the morphological and physiological events occurring after sectioning one of the pair of octopus' pallial nerves was provided [14,21]. Subsequent studies provided additional insights [22-24].

O. vulgaris possesses a pair of pallial nerves, one for each side of the mantle; these originate from the palliovisceral lobe located at the posterior end of the subesophageal mass, a part of the central nervous system [15,25]. Each of the nerves runs inside a "muscular bridge", as originally described by Sereni [18], facing the internal cavity of the mantle and ends in the stellate ganglion. Each ganglion gives rise to stellar nerves, which in turn innervate the mantle (Fig. 1a, b).
Each nerve fiber in the pallial nerve is enveloped by connective tissue sheaths; an additional outer connective layer enwraps the whole nerve [18,21,26]. Here we do not provide a throughout description of ***i.*** the organization of fibers in the pallial nerve [15,25], and ***ii.*** the structure and organization of the stellate ganglion [21,27,28] of *O. vulgaris*.
Through the innervation of muscles and chromatophores, each pallial nerve provides neural network control for breathing and skin patterning on the ipsilateral side of the mantle.

The transection of a nerve leads to immediate paralysis of respiratory mantle muscle on the denervated side, chromatophore relaxation and consequent paling of the mantle [14,18,29]. The complete regeneration of the pallial nerve and functional recovery require approximately three to four months [14].

Here we describe the sequence of events occurring after complete transection of *O. vulgaris* pallial nerve within the first 14 days after lesion. Functional recovery is observed taking into account behavioral effects of the lesion. Degeneration and regeneration are evaluated in the same individual by comparing the two pallial nerves: one post-lesion, and the contralateral one exposed and left intact, thus serving as sham control. We also describe the cellular events linked to nerve regeneration, the existence of inflammatory events, cell proliferation and the first signs of functional recovery.

Results

All animals behaved normally and did not exhibit any sign of distress or suffering after surgery [30-32] and during the following 14 days post-lesion (p.l.). Octopuses attacked their prey promptly in less than 30 seconds in all occasions exhibiting their normal predatory behavior [33-35] and fed regularly.

Behavioural patterns

A full attack response [3,36] was observed as response to the presentation of a crab as natural prey [33,35]. The effects of the damage due to the lesion appeared mostly on the mantle, ipsilateral to the lesioned side, as deficits in the full expression of body patterns exhibited by the animal.

After surgery, the lesioned side appeared 'pale' [3,29] and no control of chromatic and textural pattern resulted evident (Fig. 1c, and Fig. 2c). The contralateral side retained the ability to perform the full range of body patterns as in a normal behaving animal [3,36-39]. A few hours after recovery from anesthesia some animals showed self-grooming actions [40] consisting in arm bending over the head and the mantle surface [3]; grooming was exhibited in proximities of the denervated area and inside the mantle cavity.

One to two days later, light brown spots appeared on a white-greyish/pale background while three to five days post lesion the whole dorsal area of the denervated skin had a uniform colored appearance (Fig. 2d). Smooth skin texture was always observed in this phase.

In our experimental conditions, and contrary to what was previously described [14], starting from seven days p.l. the animals exhibited at rest a marked ability to match the chromatic pattern of the uninjured side (Fig. 2e, f). Normal chromatic patterning was not observed on the mantle while the octopus performed an attack response; in these occasions the lesioned side became again pale.

In addition, we observed an impairment of the mantle contractions during normal breathing on the denervated side, with mantle muscle activity appearing jerky and unsynchronized. We did not notice improvement during the 14 days of this study in the capability of the mantle to contract on the lesioned side during breathing, despite the fact that muscular tone improved with time. We did not recognize any additional alterations in physiological outcomes due to the altered breathing motion, and no other evident bias in the motor patterns was detected in any octopus utilized in this experiment.

At sacrifice, anesthetized animals showed dark waves appearing apparently uncontrolled on a white-grayish background on the denervated area. These waves have been observed by Packard [41] and referred as “wandering clouds”. They have been considered as due to hyper-excitability of the radial muscles of chromatophores [14,18,42] and appear not to be under the control of the central nervous centers [19]. In addition, in the same conditions the denervated skin resulted to be very susceptible to mechanical stimuli contracting intensely, compared to the contralateral side which did not respond to stimulation.

Hemocyte infiltration

Large hemorrhagic areas were observed in the damaged connective tissue and muscle lesioned to expose the pallial nerves of both sides. This was probably due to the breakage of vessels that run along the pallial nerve [43]. Scar tissue appeared in all the injured areas, i.e. muscles, connective and nerve tissues, even though the extent of the cicatricial tissue in the sham control appeared minimal relative to the scars formed post lesion (Fig. 3, and Fig. 4).

Three days after surgery a thick scar appeared separating the cut ends of the nerve (Fig. 3a, b). Fourteen days post lesion a large reduction of the size of the scar was observed.

The scar impeded the two stumps to come into contact (Fig. 3a). However, this did not represent a permanent barrier for the axons outgrowth. Regenerating fibers from the central stump appeared growing into the scar toward the peripheral stump within seven days post lesion (Fig. 3f).

We calculated the size of the scar by counting the number of cells both in the the sham control nerve and at the same level in the lesioned nerve. At three days p.l. we found an average of 950 cells per stack (CL), while in the lesioned nerve this number appeared to be about three times higher (LL: 3000 cells per stack; p = 0.043 after Student's *t*-test; Fig. 6a). The number of cells forming the scar decreased to around 1800 cells per stack (LL) a week after injury (7 days p.l.) in the lesioned area, a number that appeared to be still different from the cells counted in control areas (CL: 1100 cells; p < 0.001 after Student's *t*-test). Finally, a significant increase of the number of cells in respect to the controlateral area was observed in the peripheral side of the lesion (14 days p.l.; L_P1 and L_P2: 1900 and 2000 cells respectively; C_P1 and C_P2: 950 cells; L_P1 vs C_P1, p < 0.001; L_P2 vs C_P2, p = 0.019 after Student's *t*-test; Fig. 6a).

The contribution of hemocytes to scar resulted not quantifiable under our experimental conditions. However, these appear to be the larger component. In fact, several cells identified by morphology as hemocytes contributed to scar formation at the lesion site (LL) and infiltrated between regenerating fibers of the central stump (Fig. 3b, e).

Numerous hemocytes also infiltrate the peripheral stump in contact with regenerating fibers at 14 days p.l.; these were not evident at earlier time-points in this area. Within the scar they appeared to undergo structural changes from the classical spherical form they retained in the vessels, to a spindle shape when they reached the site of lesion (Fig. 3b). This observation is compatible with those reported by Féral [44] during arm regeneration in the cuttlefish (*Sepia officinalis*) in which hemocytes (i.e. blood cells) migrated to the wound to form the blastema.

Degeneration* vs *axonal regrowth

Regeneration occurred differently between the central and peripheral nerve stumps. The central stump was characterized by intensive axon growth already three days after surgery. On the other hand, the peripheral stump of the nerve towards the stellate ganglion showed mainly degenerative processes. The main axonal re-growth was observed in the proximal area of the central stump (Fig. 3a, b; areas corresponding to L_C2 in Fig. 1) with fibers oriented in many different directions, revealing a disorganized pattern. The majority of the regenerating nervous fibers led toward the scar tissue, though some of them penetrated the scar. The leading connective tissue still appeared not formed (Fig. 3b). The peripheral stump closest to the injury site was degenerating and we observed axons breaking in lumps, as originally described by Sereni [18].

Seven days p.l. the outer connective tissue enveloping the nerve tightened around the cut stumps (Fig. 3d; corresponding to areas L_C2 and L_P2 close to the lesion in Fig. 1), apparently narrowing the nerve. Regenerating fibers at the level of the central stump continued growing in multiple directions, but most of them were observed to move past the cicatricial tissue, contacting the peripheral axons (Fig. 3e, f). Axon breakage in the peripheral stump involved a larger area than the previous stage (Fig. 3g). Multiple lumps formed by debris of degenerating axons appeared to be swollen. Neurofilaments (detected by NF200 antibody) appeared to accumulate towards these swollen neuronal terminal endings.

Significant changes in the nerve regeneration process were observed two weeks after the injury. At this time point, we observed a retraction of at least one of the two stumps, probably consistent with degeneration of the peripheral stump. This produced an apparent increased distance between the two stumps, compared to the first time-points investigated.
We observed numerous fibers directed toward the peripheral stump appearing well organized and forming a defined spike-like structure within nascent connective tissue (Fig. 3h). Nevertheless, the neural fibers in the central stump still generally showed a disorganized appearance. In the opposite stump, degeneration was still evident, although, many regenerating fibers protruded for several microns within the debris. These fibers appeared well-organized in bundles enveloped by connective tissue (Fig. 3i).
In all cases the two stumps were directed toward each other and made contact.

Regeneration/degeneration phenomena observed at the different time-points were also identified by considering the area occupied by the neuronal filaments. The major changes where observed in the lesioned nerve at the level of the central stump (L_C2) seven days post lesion (L_C2 vs C_C2 neurofilament area, $p < 0.001$ after Student's *t*-test; Fig. 6b) due to axonal regrowth in the central stump (Fig. 3a, d). Degeneration resulted in considerable axonal loss when compared with controlateral nerve (see Fig. 4), revealing a reduced neurofilament area (L_P2 vs C_P2, 3 and 7 days p.l., $p < 0.010$ after Student's *t*-test; Fig. 6b).
Fourteen days after lesion a similar situation was found in the lesioned nerve at the level of the peripheral (L_P2) stump (neurofilament area, lesioned vs controlateral side, $p = 0.001$ after Student's *t*-test), but not when the central stump was considered (L_C2 vs C_C2, $p = 0.924$, NS after

Student's *t*-test). In the sham controls a constant number of fibers were detected at both sides (i.e. central vs peryphery) and corresponding locations (Fig. 6b).

Cell proliferation

Large numbers of hemocytes were observed three days post injury contributing to the formation of the scar tissue between the two stumps. They also provided the main source of proliferating cells found at this time-point (Fig. 5a-e). We counted 20 PHH3 positive cells (from a total of 3000 per stack) at the lesioned site (LL, Fig. 6c; Number of PHH3 cells at LL vs CL: $p = 0.008$ after Student's *t*-test). Mitotic hemocytes were also found within the blood vessel running into the central stump, leading to the injury and at the level of the connective tissue surrounding the nerve (Fig. 5b; number of PHH3 cells at L_c2 vs C_C2: $p < 0.001$ after Student's *t*-test). The sham control showed some proliferating cells in the external connective layer, but no proliferating hemocytes were detected inside the nerve or in the inner blood vessels (Fig. 4, and Fig. 6c).

Seven days after injury the number of proliferating cells remained similar (PHH3 *vs* total cells: 25, 1900 cells per stack, LL vs CL: $p = 0.001$ after Student's *t*-test) to the number observed during the previous time-point. PHH3 positive cells did not appear restricted to the lesioned site, but rather were expanding towards new growing fibers (L_C2, PHH3 vs total cells per stack: 46, 1500 respectively; L_c2 vs C_C2, $p = 0.001$ after Student's *t*-test; Fig. 5f, and Fig. 6c). At the same time-point we also observed other proliferating cells with morphological features typical of the connective tissue. These were characterized by larger elongated nuclei and were positioned within the tissue around nerve fibers (Fig. 5i).

Similar cells occasionally appeared in the sham control nerves and in uninjured nerve (data not shown), suggesting a basal level of proliferation of the connective tissue. However, these numbers were low compared to the injured nerve. We found on average zero to three proliferating cells per stack in the sham nerve (Fig. 4), and between zero and one in the uninjured nerve.

A large number of proliferating cells were found inside the lesion site 14 days after injury (PHH3 *vs* total cells: 25, 1800 cells per stack; LL vs CL $p < 0.001$ after Student's *t*-test). A similar number was also detected in the peripheral stump (PHH3 positive *vs* total cells per stack, L_P2: 28, 2000; L_P1: 6, 1900; $p = 0.009$ after Student's *t*-test; Fig. 5k, and Fig. 6c). The great majority of these cells were identified as connective tissue-like cells and hemocytes.

Finally, we detected proliferating cells at the level of the peripheral stump. These were also positively marked with the neuronal marker NF200. These cells appeared to be scattered between both degenerating and regenerating fibers (Fig. 5l, m).

Some mitotic cells appearing within the external connective layer were also positive for NF200. The latter were identified at all the time-points in both the injured nerve (Fig. 5h, j) and the sham control.

In any case, no NF200-positive cells were ever found inside the control nerve.

Discussion

Our findings extend those previously reported to occur after *O. vulgaris* pallial nerve lesion and subsequent regeneration (Table 1). After complete transection of the pallial nerve hemorrhagic areas appearing on the lesioned side were immediately followed by cicatricial tissue formation. A scar is formed between the two stumps, but it does not represent an inhibitory environment to the nervous fibers that start to regenerate from the central stump and cross the injury site to reach the peripheral side. Although the nature of scar cells remains unknown, we were able to recognize hemocytes as the primary contributors of scar tissue. They were identified by their characteristic round shape and u-shaped nuclei (Fig. 5d), and appeared to originate by the damaged vessels during surgery.

The intense vascularization in the vicinity of pallial nerves [43] supports this view. The stellate ganglia are supplied by right and left pallial arteries that branch from the anterior aorta and that run dorsally to two pallial veins. In addition, a blood vessel runs within the pallial nerve itself, and likely contributed to hemocytes release in the area of injury.

Hemocytes are the only cell type reported in the circulating hemolymph of *O. vulgaris* and they possess phagocytic activity [45,46], thus supporting the view that their presence in areas closed to the lesion, and between degenerating and regenerating neuronal fibers, may in part be related to active debris removal, as originally observed by Sereni [18].

As schematized in Figure 7, hemocytes have a leading role in the regenerative process of the pallial nerve. They first migrate to the lesion site and spread among scar and regenerating fibers of the central stump. Mitotic hemocytes are recruited to the lesion through systemic blood circulation, travelling into the blood vessel inside the central stump. No mitotic hemocytes were found in the contralateral nerve, thus suggesting that some chemo-attractive signals are released in the site of

lesion and are responsible for attracting proliferating hemocytes as described by Féral [44]. Interestingly, these signals apparently cannot be triggered by a generic insult (e.g. muscles or connective tissue lesion), but require injury of the nerve or of the blood vessel running inside the nerve, as proven by the fact that in sham controls, where the nerve was approached, but left intact, mitotic hemocytes were not found. Also consistent with a regenerative role for hemocytes is the fact that proliferating blood cells are initially found mainly in the central stump, where a substantial tangle of new fibers is growing. In the opposite stump little sign of regeneration is visible and the number of proliferating hemocytes is more restricted. It is possible that hemocytes may release factors that foster regeneration of axons; this assumption seems to be further supported by the fact that at 14 days after lesion numerous mitotic hemocytes are found among regenerating fibers of the peripheral stump.

In parallel, mitotic cells belonging to connective tissue also appear soon after nerve lesion. Their number also increases with time, following a similar pattern of compartmentalization of hemocytes: first in the central stump and only later in the periphery.

In the last time-point observed (14 days post lesion), mitotic cells positive for neurofilament marker were found among the degenerating fibers and regenerating bundles of the peripheral stump (Fig. 5l, m). Although their nature and function is still unknown, the expression of neurofilament marker in these cells might indicate a process of differentiation of unlabeled stem/progenitor cells (or glial cells) present at the early stages of pallial nerve regeneration. Connective tissue cells of the external layer also proliferate and express NF200 marker, thus supporting the view that glial cells might be involved in the process.

In the sham control, the nerves showed no morphological alterations and just a few mitotic cells; these were primarily in the outer connective tissue.

Axon outgrowth in the central stump after complete transection is quick and, at least initially, very disorganized. Old outer connective tissue tightens around the cut nerve ends while inner connective sheaths do not grow together with regenerating fibers. Only later, organized connective sheaths wrap fibers, forming a spike-like structure in the central stump, directed toward the peripheral stump. Fibers of the peripheral stump, instead, degenerate and form debris, which gradually extend in the nerve from the site of lesion toward the stellate ganglion. A few days later, the peripheral this stump shows evident signs of regeneration, with new fibers growing into fascicles and tightly enwrapped in connective tissue (Fig. 7). Detection of NF200-positive

proliferating cells at the level of the peripheral stump and between degenerating and regenerating fibers suggests that neuronal stem/progenitor cells also contribute to nerve regeneration.

Thus nerve regeneration in the octopus involves at least *i.* axonal re-growth and *ii.* neuronal stem/progenitor cell proliferation and differentiation.

As summarized in Table 1, we observed partial functional recovery between seven and 14 days post lesion in contrast to what reported by previous studies [14,18]. This recovery pertains only to skin pattern and not breathing due to impaired mantle contraction. Indeed, while the animals showed again some ability in modulating chromatophore contraction/relaxation, mantle muscles contraction remained inhibited at the level of the lesioned side. This might be explained by a local control of chromatophores, exerted by light on skin receptors rather than re-innervation of target tissues, as already suggested by Packard and Brancato [47] .

Unlike the response of mammalian spinal cords to injury, where a glial scar forms and structural reconnectivity is inhibited [48], several aspects of the observed response in octopuses mirror the regenerative response of mammalian peripheral nerves, which, following crush injury or acute transection and repair, is often successful.

The response of peripheral nerves to injury has been well-characterized [49-51]. Briefly, several structural and biological changes occur in the severed nerve stumps within 1-3 days of injury, including cytoskeletal destabilization and organelle accumulation in the proximal stump, and Wallerian degeneration in the distal stump. The primary structural changes to the distal stump are the loss of nerve fibers and dedifferentiation and compaction of Schwann cells and basal lamina into Bands of Büngner [52-56]. Also present in these bands are various proteoglycans and an organized (non-fibrotic) collagenous matrix, which collectively provide well-organized tracks for regenerating axons. Proximal stump outgrowth, axonal sprouting, and extension begin within 3-5 days following injury, and axons that extend into the distal stump within 1-2 months thus experience a highly favorable regenerative environment, which is further enhanced by increased Schwann cell expression of chemoattractive growth factors and their receptors [57,58]. While Bands of Büngner are not readily apparent in the regenerating octopus pallial nerve, the progressive increase in structural organization in the early days following injury suggests the creation of a favorable structural environment for axonal regrowth. Importantly, in both models, as proximal axons enter the distal stump, normal structure is restored in the vicinity of regenerating axons.

In parallel to structural changes, degenerating mammalian nerves also experience the infiltration of a variety of cells at the injury site. Indeed, bone-marrow macrophages reach the site of lesion in a few hours, and within one to two days, macrophages are recruited from systemic circulation, attracted by inflammatory cytokines and chemokines released by resident macrophages [49]. Among other functions, these macrophages are responsible for sequestering and eliminating or recycling myelin debris, which appear to be the role of hemocytes in *O. vulgaris*.

Compellingly, recent work also suggests an important role for stem/progenitor cells, which may be recruited from surrounding muscle or the vasculature, in improving nerve regeneration [59]. Proliferation and conversion of these cells into nerve cells such as Schwann cells appears to be an essential aspect of the regenerative response, and may represent conceptual similarity with proliferating connective tissue cells observed in the octopus.

Cumulatively, then, successful repair in both octopus and mammals appears to be guided by effective innate-immune response and the timely intervention of Schwann cells, fibroblasts, endothelial cells, and the molecules they produce [49,60,61].

Although further investigation is required to better characterize the regenerative process in octopuses, these results represent an important starting point to understand the mechanisms involved in nerve regeneration in *Octopus*. Hemocytes and connective tissue cells contribution was described here to greater extent than original observations by Sereni and Young [18], underlining the involvement of immune cells and glia for *O. vulgaris* as occurs in all vertebrate models of nerve regeneration. Two weeks, indeed, appear sufficient to organize and build the directional and leading scaffolding in both stumps, allowing them to grow toward each other, overcome the scar and, in some cases, to obtain a partial recovery of the chromatic function. We cannot exclude that the functional recovery of the body patterning in the octopus maybe also facilitated by phenomena (e.g. local network control) not necessarily related to structural regeneration, as suggested by Packard and Brancato [47].

Materials and Methods

Animals

Adult *Octopus vulgaris*, both sexes (body weight: 250-350 g; N = 12, ♂ = 5 ♀ = 7) caught from the Bay of Naples were kept under standardized conditions [35,62] in the laboratory. Experiments were conducted during spring of the 2013 (sea water temperature range: 18-20 °C). All the animals were fed with crabs once a day. Octopuses for this study were selected for the absence of any regenerating sign or any kind of lesion, and appearing exploratory driven and healthy [33,34]. Experiments with live octopuses were carried out before transposition of Directive 2010/63/EU in Italy. Although no authorization was required, all procedures were performed in order to minimize the pain and distress of the animals involved [30-32,63].

Nerve transection

O. vulgaris were anesthetized by immersion in 3.5% $MgCl_2$ in sea water for 15 minutes, which produced complete relaxation and immobility of the animals [64]. Anesthetized animals were placed on a surgery table, positioned on a dissecting tray containing the anaesthetic solution. Octopuses were turned on their ventral side, the mantle slightly overturned to expose the nerve and the stellate ganglion nearby; a scalpel was used to make an incision on the internal side of the mantle cutting the skin, muscle and connective tissue enwrapping the pallial nerves. In this way both nerves (left and right side of the animal) were exposed using a skin hooklet. To standardize the site of the injury along the nerve, the diameter of stellate ganglion was measured for each animal, and the same length computed as distance along the nerve to set the site of severing. Left-side nerve remained intact and gently positioned back on its natural position thus serving as a sham control. The right-side pallial nerve was hold with the hook and completely transected using fine scissors. The entire operation lasted less than five minutes.

The completeness of the transection was verified by visual inspection under a stereo microscope. Uninjured samples belonging to other three animals were also collected to assess the effect of lesion on tissues surrounding the nerve.

Following surgery the animals were returned to their tanks and allowed to recover [64,65]. Full recovery was based observing re-acquisition of the normal posture, regular breathing rate and return to den; this usually requires less than 30 minutes, and a full predatory response was recorded 60 minutes later [31,66].

Behavioral observations and animals care

After recovery, octopuses were maintained in experimental tanks and fed on live crab (*Carcinus maenas*) every day following procedures described in Amodio et al. [35]. Predatory responses were videorecorded by remote controlled digital video cameras (Panasonic HDC-SD80), which were hidden from each animal's view. Each presentation lasted a maximum of two minutes (ceiling latency to attack: 121 s) and a failure to attack within this period was classified as "no attack" [33,35,62]. Behavioral observations were carried out at the same time of the day, in the afternoon. Video recordings of operated animals were examined to analyze behavior and to detect changes in octopus appearance between the lesioned and the control sides. In particular, chromatic and textural patterns were noted daily during the attack behavior and at rest, for at least 10 minutes before and after the prey presentation in the octopus tank.

From video-recordings, two independent observers deduced ***i.*** the latency to attack the prey; ***ii.*** the body pattering and the approximate areas of blanching of the skin (mantle and any other body part) according to the descriptions provided by other authors [14,22,23]. Body patterning observed during the analysis of video-recordings was coded following Borrelli et al. [3]. Behavioral observations also served as assessment of health and welfare of animals according to principles stated in Directive 2010/63/EU; Signs based on appearance, behavior and physiology were searched from a checklist as part of health monitoring program and eventually recorded [32].

Collection of samples and humane-killing of octopuses

Animals were humanely killed at three different time-points: three, seven and 14 days after injury. At the selected time-points the octopuses were deeply anesthesized (> 30min) by immersion in a 3.5% solution of magnesium chloride hexahydrate in seawater; death was confirmed by transection of dorsal aorta [32,64].

On the surgery pad, a clamp was used to pinch and hold the pallial nerve during harvesting. Both pallial nerves (cut and sham or control) were collected together with the stellate ganglion and surrounding tissues.

Frozen and paraffin sections

Samples were fixed in paraformaldehyde (4% PFA in sea water; for 1h 30 min), washed in PBS (pH 7.4) and rinsed over night at 4°C. They were cryoprotected in sucrose (30% in PBS; pH 7.4) until tissue sinking, and frozen using tissue freezing and blocking medium (OCT; Leica Biosystems). Longitudinal 30 µm thick slices were obtained using a cryostat (Leica CM3050 S). For paraffin

sections, samples were dehydrated through an ascending series of alcohol, cleared in xylene, immersed in paraffin and then cut into 5 µm thick sections.

Immunohistochemistry and histology

Cryostat sections were used for immunohistochemistry. They were air dried for 1h, washed in PBS and Normal Goat Serum (NGS) 5% in PBT (PBS + Tween 0.1%) was used as a blocking agent. Slices were then incubated with primary antibodies, diluted in NGS 1% in PBT overnight at 4°C. Anti-Neurofilament 200 Sigma N5389 (NF-200, 1:2000), and anti-Phospho-Histone H3 Sigma H9908 (PHH3; 1:600) to label axons and detect cell proliferation, respectively were utilized. Sections were then washed with PBT and then incubated with secondary antibodies (1:250; respectively Alexa Fluor goat anti-mouse IgG1 594, and Alexa Fluor goat anti-rat IgG (H+L) 488) for 1h at room temperature. The omission of each primary antibody was used as negative control for each immunostaining. Following washing in PBT, DAPI (diluted 1:1000 in PBS) was used to counterstain nuclei. Paraffin sections were stained for Masson's trichrome [67] after paraffin removal and rehydration in an ethanol series.

Confocal imaging

Sections labeled with fluorescent dyes were imaged on a Zeiss LSM 710 laser scanning confocal microscope using a 20× air objective. Z-stacks of five areas of the damaged nerve were taken.

The analysis of the events occurring after surgery focused on five areas for each pallial nerve (Fig. 1): the site of lesion (LL), a distal and a proximal area in the central stump (respectively identified as L_C1 and L_C2), and in the peripheral stump (L_P1 and L_P2) of the transected nerve. Analogous areas were identified in the control nerve preparation: corresponding lesion site (CS), a distal and a proximal area in the central 'stump' (C_C1, C_C2), and at the level of the peripheral 'stump' (C_P1, and C_P2).

Morphology and anatomical description

We follow morphological and event descriptions as provided by Young and coworkers [15,18,21,25]. The two stumps have been identified as belonging to central and peripheral sides of the pallial nerve, respectively. According to modern literature on nerve regeneration, these should be named respectively proximal and distal, but here we refer to the classic terminology.

Image and Data analysis

Images were processed with IMARIS 64 7.5 (Bitplane Inc.) for nuclear and mitotic cells counting and neurofilament area calculation. Statistics and box-and-whisker plots were generated using SPSS version 14.0 (SPSS Inc). Data were tested for normality and Student's t-test was applied according to Zar [68]. Differences were considered significant at $p < 0.05$.

Acknowledgments

This work is part of the PhD project of Pamela Imperadore (PhD program in Life Sciences, curriculum Animal Biology - Università della Calabria, Rende, Italy). The PhD program in Life Science is part of Training & Education initiatives of the Association for Cephalopod Research-CephRes. Authors are grateful to Dr Giovanna Ponte who provided valuable guidance and mentoring to PI in various phases of this project.

Competing interests

The authors declare no competing financial interests.

Author contributions

PI carried out all experiments, analyzed the data, and drafted the manuscript. HPM contributed to the experimental design; HPM and SS helped in drafting the manuscript. GF designed the experiments and revised the final manuscript. All Authors contributed to the final writing of the manuscript.

Funding

This work was supported by a grant from the Association Francaise contre les Myopathies and the National Institute of Health/National Eye Institute (NIH/NEI, Bethesda, MD, USA; Grant: 1R01EY026202) to HPM, and by the Stazione Zoologica Anton Dohrn (Napoli, Italy) and the RITMARE Flagship Project (SP2-WP4-A3; MIUR & CNR, Italy) to GF. PI is supported by the Association for Cephalopod Research-CephRes.

References

1. Young, J. Z. Computation in the learning system of cephalopods, *Biol Bull* **180**, 200-208 (1991).

2. Nixon, M. and Young, J. Z. *The Brains and Lives of Cephalopods* (Oxford University Press, Oxford, UK, 2003).

3. Borrelli, L., Gherardi, F., and Fiorito, G. *A Catalogue of Body Patterning in Cephalopoda* (Stazione Zoologica A. Dohrn; Firenze University Press, Napoli, Italy, 2006).

4. Borrelli, L. and Fiorito, G. "Behavioral Analysis of Learning and Memory in Cephalopods," in *Learning and Memory: A Comprehensive Reference,* edited by Byrne, J. J. (Academic Press, Oxford, UK, 2008), pp.605-627.

5. Lange, M. M. On the regeneration and finer structure of the arms of the cephalopods, *J Exp Zool* **31**, 1-57 (1920).

6. Polglase, J. L., Bullock, A. M., and Roberts, R. J. Wound-Healing and the Hemocyte Response in the Skin of the Lesser Octopus *Eledone cirrhosa* (Mollusca, Cephalopoda), *J Zool* **201**, 185-204 (1983).

7. Dingerkus, G. and Santoro, E. D. Cornea regeneration in the Pacific giant octopus, *Octopus dofleini*, and the common octopus *O. vulgaris*, *Experientia* **37**, 368-369 (1981).

8. Rohrbach, B. and Schmidtberg, H. *Sepia* arms and tentacles: model systems for studying the regeneration of brachial appendages, *Vie Milieu* **56**, 175-190 (2006).

9. Tressler, J., Maddox, F., Goodwin, E., Zhang, Z., and Tublitz, N. Arm regeneration in two species of cuttlefish *Sepia officinalis* and *Sepia pharaonis*, *Inv Neurosci* **14**, 37-49 (2013).

10. Bush, S. L. Autotomy as a deep-sea squid defense, *Integrative and Comparative Biology* **46**, E19 (2006).

11. Bush, S. L. Economy of arm autotomy in the mesopelagic squid *Octopoteuthis deletron*, *Marine Ecology Progress Series* **458**, 133-140 (2012).

12. Fossati, S. M., Carella, F., De Vico, G., Benfenati, F., and Zullo, L. Octopus arm regeneration: Role of acetylcholinesterase during morphological modification, *J Exp Mar Biol Ecol* **447**, 93-99 (2013).

13. Florini, M., Fiorito, G., Hague, T., and Andrews, P. L. R. "Monco": A Natural Model for Studying Arm Usage and Regeneration in *Octopus vulgaris*, *J Shellfish Res* **30**, 1002 (2011).

14. Sanders, G. D. and Young, J. Z. Reappearance of Specific Colour Patterns after Nerve Regeneration in *Octopus*, *Proceedings of the Royal Society of London Series B Biological Sciences* **186**, 1-11 (1974).

15. Young, J. Z. *The anatomy of the nervous system of Octopus vulgaris* (Oxford University Press, London, UK, 1971).

16. Callan, H. G. The absence of a sex hormone controlling regeneration of the hectocotylus in *Octopus vulgaris* L, *Pubbl Staz Zool Napoli* **18**, 15-19 (1940).

17. Dingerkus, G. and Santoro, E. D. Cornea regeneration in the Pacific giant octopus,*Octopus dofleini*, and the common octopus,*O. vulgaris*, *Experientia* **37**, 368-369 (1981).

18. Sereni, E. and Young, J. Z. Nervous degeneration and regeneration in Cephalopods, *Pubbl Staz Zool Napoli* **12**, 173-208 (1932).

19. Sereni, E. Fenomeni fisiologici consecutivi alla sezione dei nervi nei cefalopodi, *Boll Soc It Biol Sperim* **4**, 736-740 (1929).

20. Young, J. Z. Fenomeni istologici consecutivi alla sezione dei nervi nei cefalopodi, *Boll Soc It Biol Sperim* **4**, 741-744 (1929).

21. Young, J. Z. The Organization of a Cephalopod Ganglion, *Philosophical Transactions of the Royal Society of London B: Biological Sciences* **263**, 409-429 (1972).

22. Packard, A. Uses of nicotine to follow denervation supersensitivity in unilaterally denervated octopus in vivo, *J Physiol* **438**, 325 (1991).

23. Packard, A. "Through the Looking-Glass of Cephalopod Colour Patterns," in *Behavioural Brain Research in Naturalistic and Semi-Naturalistic Settings,* edited by Alleva, E., *et al.* (Kluwer Academic, Dordrecht, 1995), pp.105-130.

24. Packard, A. "Organization of Cephalopod Chromatophore Systems: a Neuromuscular Image-Generator," in *Cephalopod Neurobiology,* edited by Abbott, N. J., Williamson, R., and Maddock, L. (Oxford University Press, Oxford, 1995), pp.331-367.

25. Budelmann, B. U. and Young, J. Z. Central pathways of the nerves of the arms and mantle of *Octopus*, *Philos Trans R Soc Lond B* **310**, 109-122 (1985).

26. Young, J. Z. Memoirs: On the Cytology of the Neurons of Cephalopods, *Journal of Cell Science* **s2-75**, 1-47 (1932).

27. Monsell, E. M. Cobalt and horseradish peroxidase tracer studies in the stellate ganglion of octopus, *Brain Res* **184**, 1-9 (1980).

28. Monsell, E. M. The organization of the stellate ganglion: a study of synaptic architecture and amacrine neurons in octopus. PhD Dissertation, Duke University, 1977.

29. Fredericq, L. Recherches sur la Physiologie du poulpe commun, *Archives de Zoologie expérimentale et générale* **7**, 535-583 (1878).

30. Fiorito, G.*, et al.* Cephalopods in neuroscience: Regulations, Research and the 3Rs, *Invert Neurosci* **14**, 13-36 (2014).

31. Andrews, P. L. R.*, et al.* The identification and management of pain, suffering and distress in cephalopods, including anesthesia, analgesia and humane killing, *J Exp Mar Biol Ecol* **447**, 46-64 (2013).

32. Fiorito, G.*, et al.* Guidelines for the Care and Welfare of Cephalopods in Research - A consensus based on an initiative by CephRes, FELASA and the Boyd Group, *Lab Anim* **49**, 1-90 (2015).

33. Maldonado, H. The positive learning process in *Octopus vulgaris*, *Z Vgl Physiol* **47**, 191-214 (1963).

34. Hochner, B., Shomrat, T., and Fiorito, G. The octopus: a model for a comparative analysis of the evolution of learning and memory mechanisms, *Biol Bull* **210**, 308-317 (2006).

35. Amodio, P., Andrews, P. L. R., Salemme, M., Ponte, G., and Fiorito, G. The use of artificial crabs for testing predatory behavior and health in the octopus, *Altex-Alternatives to Animal Experimentation* **doi: http://dx.doi.org/10.14573/altex.1401282**, 1-12 (2014).

36. Packard, A. The behaviour of *Octopus vulgaris*, *Bull Inst Oceanogr (Monaco)* **1D**, 35-49 (1963).

37. Packard, A. and Sanders, G. What the octopus shows to the world, *Endeavour* **28**, 92-99 (1969).

38. Packard, A. and Sanders, G. D. Body patterns of *Octopus vulgaris* and maturation of the response to disturbance, *Anim Behav* **19**, 780-790 (1971).

39. Packard, A. and Hochberg, F. G. Skin patterning in *Octopus* and other genera, *Symp Zool Soc Lond* **38**, 191-231 (1977).

40. Mather, J. A. How do octopuses use their arms?, *J Comp Psychol* **112**, 306-316 (1998).

41. Packard, A. A note on dark waves (Wandering clouds) in the skin of *Octopus vulgaris*, *J Physiol* **446**, 40 (1992).

42. Sereni, E. The chromatophores of the Cephalopods, *Biol Bull* **59**, 247-268 (1930).

43. Isgrove, A. *Eledone* (Williams and Norgate, London, UK, 1909).

44. Féral, J. P. Wound healing after arm amputation in *Sepia officinalis* (Cephalopoda: Sepioidea), *J Invert Pathol* **52**, 380-388 (1988).

45. Castellanos-Martinez, S., Prado-Alvarez, M., Lobo-da-Cunha, A., Azevedo, C., and Gestal, C. Morphologic, cytometric and functional characterization of the common octopus (*Octopus vulgaris*) hemocytes, *Dev Comp Immunol* **44**, 50-58 (2014).

46. Cowden, R. R. and Curtis, S. K. "Cephalopods," in *Invertebrate Blood Cells. General Aspects; Animals Without True Circulatory Systems to Cephalopods,* edited by Ratcliffe, N. A. and Rowley, A. F. (Academic Press, London, UK, 1981), pp.301-323.

47. Packard, A. and Brancato, D. Some responses to chromatophores to light, *J Physiol* **459**, 429 (1993).

48. Cregg, J. M.*, et al.* Functional regeneration beyond the glial scar, *Experimental Neurology* **253**, 197-207 (2014).

49. Rotshenker, S. Wallerian degeneration: the innate-immune response to traumatic nerve injury, *Journal of Neuroinflammation* **8**, 109 (2011).

50. Navarro, X., Vivó, M., and Valero-Cabré, A. Neural plasticity after peripheral nerve injury and regeneration, *Progress in Neurobiology* **82**, 163-201 (2007).

51. Hall, S. The response to injury in the peripheral nervous system, *The Bone & Joint Journal* **87-B**, 1309-1319 (2005).

52. Bignami, A., Chi, N. H., and Dahl, D. Laminin in Rat Sciatic Nerve Undergoing Wallerian Degeneration, *J Neuropathol Exp Neurol* **43**, 94-103 (1984).

53. Goodrum, J. F., Earnhardt, T., Goines, N., and Bouldin, T. W. Fate of myelin lipids during degeneration and regeneration of peripheral nerve: an autoradiographic study, *The Journal of Neuroscience* **14**, 357-367 (1994).

54. Salonen, V., Peltonen, J., Röyttä, M., and Virtanen, I. Laminin in traumatized peripheral nerve: Basement membrane changes during degeneration and regeneration, *Journal of Neurocytology* **16**, 713-720 (1987).

55. Tona, A., Perides, G., Rahemtulla, F., and Dahl, D. Extracellular matrix in regenerating rat sciatic nerve: a comparative study on the localization of laminin, hyaluronic acid, and chondroitin sulfate proteoglycans, including versican, *Journal of Histochemistry & Cytochemistry* **41**, 593-599 (1993).

56. Salonen, V., Röyttä, M., and Peltonen, J. The effects of nerve transection on the endoneurial collagen fibril sheaths, *Acta Neuropathologica* **74**, 13-21 (1987).

57. Höke, A., Gordon, T., Zochodne, D. W., and Sulaiman, O. A. R. A Decline in Glial Cell-Line-Derived Neurotrophic Factor Expression Is Associated with Impaired Regeneration after Long-Term Schwann Cell Denervation, *Experimental Neurology* **173**, 77-85 (2002).

58. Boyd, J. G. and Gordon, T. Glial cell line-derived neurotrophic factor and brain-derived neurotrophic factor sustain the axonal regeneration of chronically axotomized motoneurons *in vivo*, *Experimental Neurology* **183**, 610-619 (2003).

59. Lavasani, M.*, et al.* Human muscle-derived stem/progenitor cells promote functional murine peripheral nerve regeneration, *J Clin Invest* **124**, 1745-1756 (2014).

60. Fawcett, J. W. and Keynes, R. J. Peripheral-Nerve Regeneration, *Annual Review of Neuroscience* **13**, 43-60 (1990).

61. Liu, K., Tedeschi, A., Park, K. K., and He, Z. G. Neuronal Intrinsic Mechanisms of Axon Regeneration, *Annual Review of Neuroscience* **34**, 131-152 (2011).

62. Fiorito, G., von Planta, C., and Scotto, P. Problem solving ability of *Octopus vulgaris* Lamarck (Mollusca, Cephalopoda), *Behav Neural Biol* **53**, 217-230 (1990).

63. Smith, J. A.*, et al.* Cephalopod research and EU Directive 2010/63/EU: Requirements, impacts and ethical review, *J Exp Mar Biol Ecol* **447**, 31-45 (2013).

64. Grimaldi, A. M., Agnisola, C., and Fiorito, G. Using ultrasound to estimate brain size in the cephalopod *Octopus vulgaris* Cuvier in vivo, *Brain Res* **1183**, 66-73 (2007).

65. Pagano, E., Ponte, G., Andrews, P. L. R., and Fiorito, G. A Comparative Analysis of Different Anaesthetics in Octopus: Towards True Anesthesia?, *J Shellfish Res* **30**, 1016 (2011).

66. Agnisola, C., Castaldo, P., and Fiorito, G. *Octopus vulgaris* (Mollusca, Cephalopoda) as a model in behavioral pharmacology: A test of handling effects, *Physiol Behav* **59**, 729-733 (1996).

67. Bancroft, J. D. and Stevens, A. *Theory and practice of histological techniques*, 2nd ed ed. (Churchill Livingstone, Edinburgh, UK, 1982).

68. Zar, J. H. *Biostatistical analysis* (Prentice Hall, Upper Saddle River, N.J., 1999).

Table 1. **An historical overview of phenomena described to occur after lesion of the pallial nerve in *Octopus vulgaris*.** The information obtained in this study is summarized here as comparison. Young [20] observed only degeneration of both stumps within the first 10 days after lesion (d), no further degenerative phenomena were reported till the end of the experiments (40 days in Young [20]). Sereni and Young [18] observed "amoebocytes" infiltration into the cut stumps, especially the peripheral one, where they appear to phagocytose actively. Young [21] reported a "vigorous" regeneration originating from the peripheral stump of the pallial nerve, and suggested this due to the afferent fibers from the periphery.

Some of the most significant events occurring after lesion of the octopus pallial nerve are described for the first time in this study.

Structure and/or Events		Young, 1929 [20]	Sereni & Young, 1932 [18]	Young, 1972 [21]	Sanders &Young, 1974 [14]	*This study*
Nerve Fibers	Degeneration	**√**	**√**	**√**	**√**	**√**
	Regeneration		**√**	**√**	**√**	**√**
Scar formation			**√**			**√**
Hemocytes	Infiltration among nerve fibers		**√**			**√**
	Proliferation		**√**			**√**
	Phagocytosis		**√**			
	Contribution to scar		**√**			**√**
Connective tissue cells	Proliferation					**√**
	Neuronal marker expression					**√**
Neuronal Cells	Presence in the nerve					**√**
	Proliferation					**√**
First signs of functional recovery of body patterning					**30d**	**7d**

Figure legends

Figure 1. Main features of the anatomy of *Octopus vulgaris* in relation to the pallial nerve, and effects of its lesion. (**a**) General anatomy of *O. vulgaris*. In red the two pallial nerves are visible rising from the posterior part of the brain, each of them directed toward the ipsilateral side of the mantle. (**b**) Enlargement of head and mantle to show the two pallial nerves ending each into a stellate ganglion. For each nerve five areas are identified for the purpose of this study, and used as target for imaging and subsequent analysis: a distal and a proximal area in the central stump (respectively identified as L_C1 and L_C2), similarly in the peripheral stump (L_P1 and L_P2) of the transected nerve. Analogous areas were identified in the control nerve, i.e.: the one corresponding to the lesion site (CL), a distal and a proximal area in the central 'stump' (C_C1, C_C2), and at the level of the peripheral 'stump' (C_P1, and C_P2). (**c**) Right pallial nerve transection causes complete paling of the mantle at the level of the denervated side due to loss of neural control of the chromatic and textural components of body patterns.

Figure 2. Behavioral patterns exhibited by octopuses following injury. (**a**) Before lesion an octopus showing normal body patterning. (**b**, **c**) Immediately after surgery the skin of the mantle of the lesioned side becomes pale (**b**; 30 min p.l.) and white (**c**; 4h p.l.**)**. Skin of the contralateral side retains the ability to perform full range of patterns as before lesion. (**d**) Three days post lesion uniform coloration is visible on dorsal area of the denerved area. (**e**, **f**) Octopuses at rest exhibit a colour pattern matching the contralateral side appearing improved with time after 7d (**e**) and 14d (**f**) after lesion.

Figure 3. Degeneration and regeneration in the pallial nerve. (**a**) Following transection of the *O. vulgaris* right pallial nerve, a scar is visible 3d post-surgery separating the two stumps (marked with yellow arrows in **a**, **b**). (**b**) Masson's trichrome staining shows scar tissue mainly formed by hemocytes which leave the blood stream and accumulate at the site of lesion (marked by asterisk). (**c**) Scar tissue and hemocytes infiltration are observed after Masson's trichrome staining in the connective tissue (in blue) and muscles (in red) after surgery required to expose the nerve. Regenerating fibers (pink) originating from the central stump appear not enveloped by connective tissue and are seen to spread in several directions (**b**) toward the scar. (**d**) Seven days (7d) post injury regenerating fibers from the central stump overcome the scar (marked with yellow arrows,

d) and penetrate the opposite stump (**e**, **f**), the latter characterized by axon breakage (**g**). (**h**) Fibers of the central stump, 14 days post injury, regenerate forming a spike-like structure driven by connective tissue toward the opposite stump which, beside showing marked degeneration, presents bundles of regenerating axons (**i**). Scale bars: 200 μm in **a**, **d-i**; **b**, **c**: 100 μm.

Figure 4. Sham control nerves. Sham lesion of left pallial nerve in octopus does not alter nerve morphology; see dotted box images for each nerve at the three time-points: (**a**) 3 days, (**b**) 7 days, and (**c**) 14 days post lesion. Hemorrhagic areas and scar tissues (marked with yellow arrows) appear in the connective tissue and muscles around the nerve, due to damage occurred to expose it during surgery. Only few mitotic cells were highlighted in sham control nerves, limited to the outer connective tissue layer (**c**). Scale bar: 200 μm; yellow dotted enlargements: 50 μm.

Figure 5. Cell proliferation. (**a-e**) In the scar tissue between the two cut stumps (marked with yellow arrows, **a**), many cells actively proliferate (green in **a-e**). (**b**) Proliferating hemocytes run inside the blood vessels which run along the pallial nerve. (**c-e**) Hemocytes are recognized by characteristic U-shape nuclei and the dimension of their nucleus. (**f, g**) Seven days post lesion hemocytes infiltrate among regenerating fibers of L_C2 and proliferate. (**i**) Cells of the connective tissue, which envelop the nerve fibers, start proliferating inside the cut nerve. (**h, j**) Cells of the outer connective layer proliferate showing neurofilament marking. (**k-m**) 14 days post lesion, mitotic cells are found among degenerating nerve fibers, some of them showing neurofilament marking (marked with yellow arrow in **k**). Scale bars: (**a, b, k**) 100 μm; (**f**) 50 μm; (**c-e**; **g-j**) 10 μm; (**l, m**) 20 μm.

Figure 6. Boxplots showing (a) **number of cells involved in scar formation,** (**b**) **nerve fibers degeneration/regeneration and** (**c**) **cell proliferation after octopus pallial nerve transection.** Three days post lesion (3d), an increase in the number of cells (**a**) is observed in LL, consisting of scar formation and hemocytes infiltration. The same area is also interested by intense mitotic activity. (**b**) L_C2 area shows a high increase in nerve fiber area due to axon regeneration at all time-points investigated, while degeneration is mainly observed in L_P2 and L_P1 14d. (**c**) Cell infiltration and proliferation inside the cut nerve is also observed in L_C2 seven (7d) and L_P2 14 days p.l. (14d).

Different areas of interest of the pallial nerve analyzed in this study are indicated (see legend in **a**); see also legend of Figure 1. See also text for detail and statistics.

Figure 7. **Graphical overview of the processes occurring following octopus pallial nerve lesion.** Hemocytes are involved in scar formation between nerve stumps; they actively proliferate in LL three days post injury. Regenerating fibers are found in the central stump, growing in several directions. Seven days after lesion fibers are able to grow across the scar toward the peripheral stump. Many connective tissue cells proliferate inside the nerve. A spike-like structure forms two weeks post injury in the central stump, due to connective tissue guide. In the peripheral stump, so far showing mainly axon degeneration, bundles of regenerating axons appear, enveloped by new forming connective tissue. See text for details.

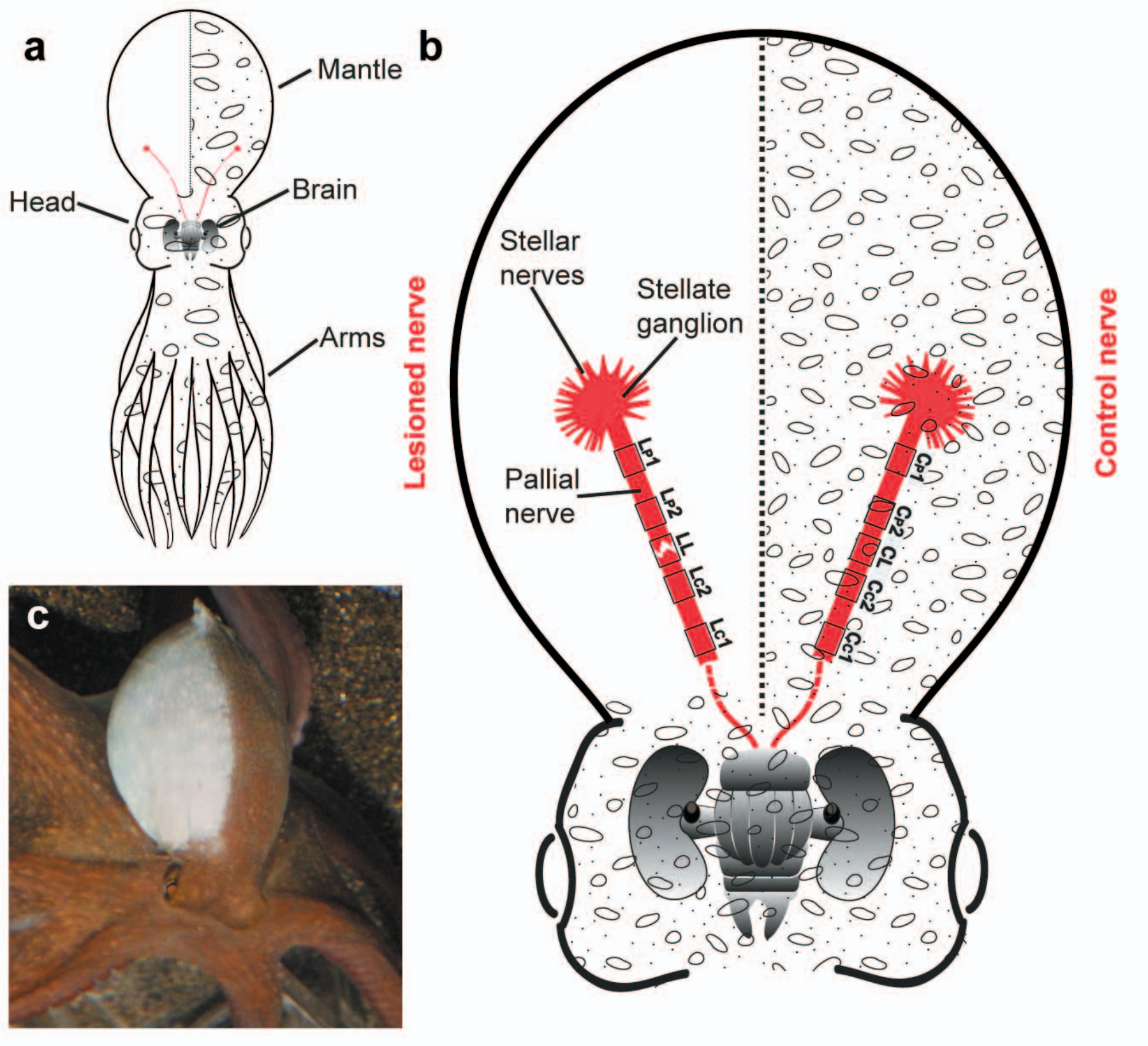
a
Mantle
Head
Brain
Arms
b
Lesioned nerve
Control nerve
Stellar nerves
Stellate ganglion
Pallial nerve
LP1
LP2
LL
LC2
LC1
CP1
CP2
CL
CC2
CC1
c

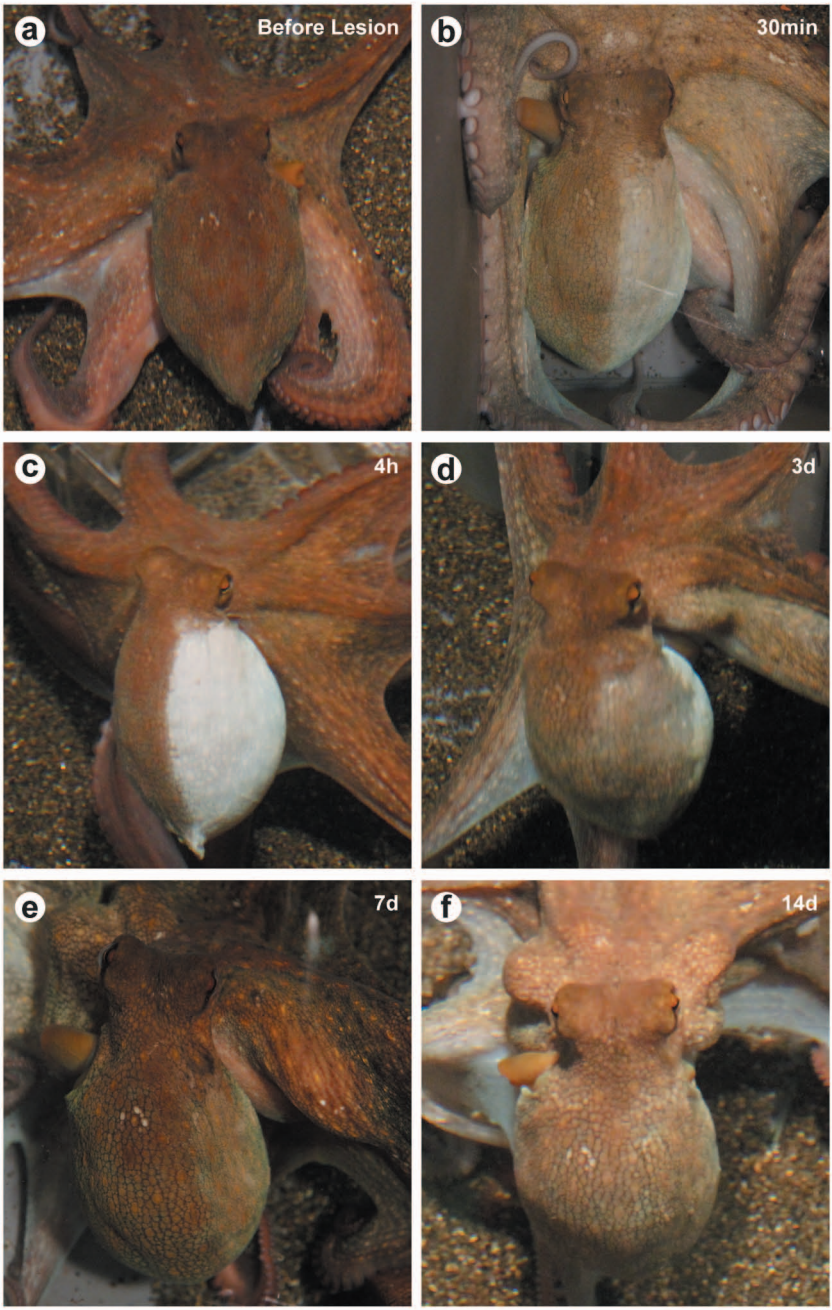
a
Before Lesion
b
30min
c
4h
d
3d
e
7d
f
14d

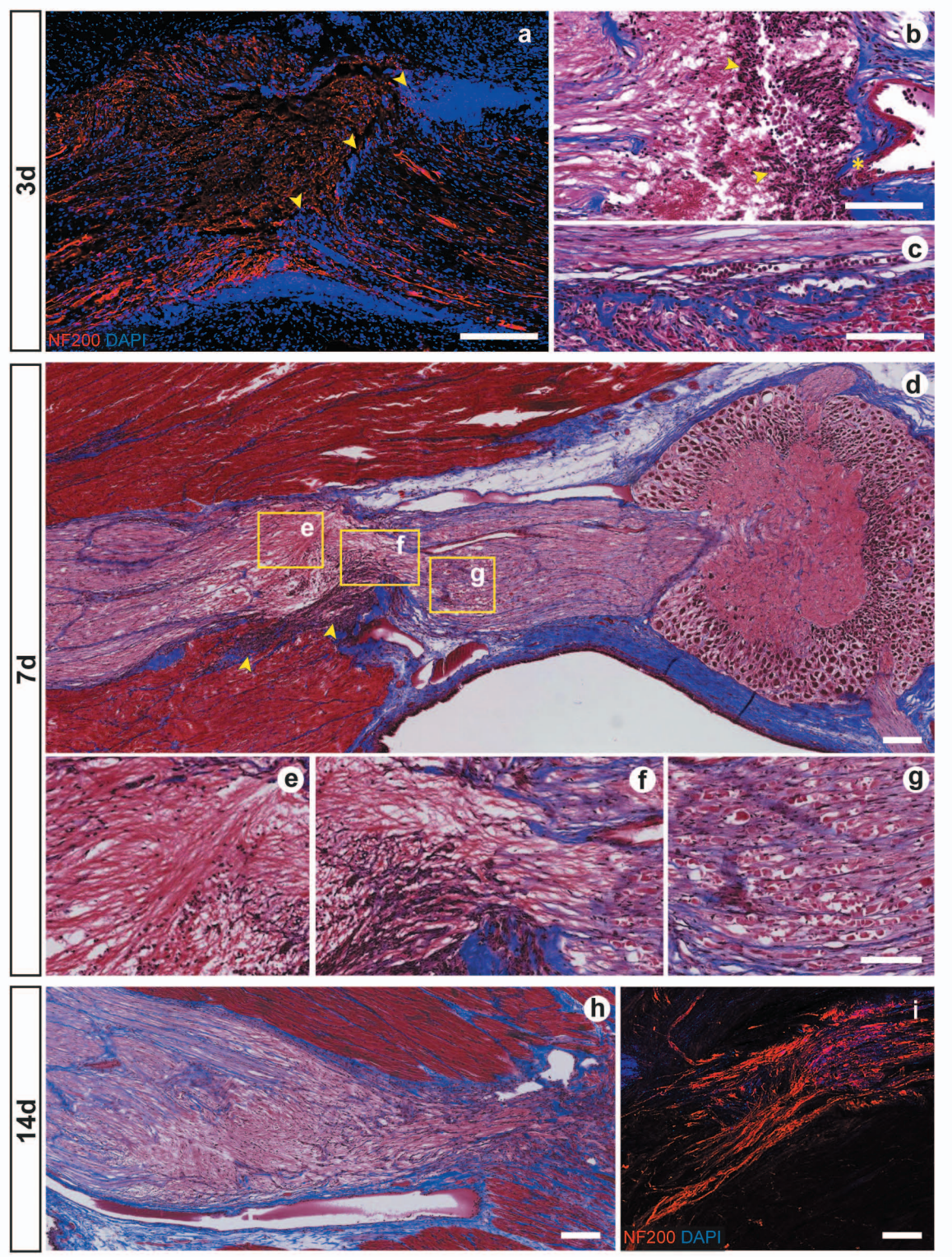
3d
a
b
c
NF200 DAPI
7d
d
e
f
g
e
f
g
14d
h
i
NF200 DAPI

3d
a
7d
b
14d
c
NF200 PHH3 DAPI

3d
a
b
c
d
e
NF200 PHH3 DAPI
PHH3
DAPI
7d
f
g
h
i
j
14d
k
l
m

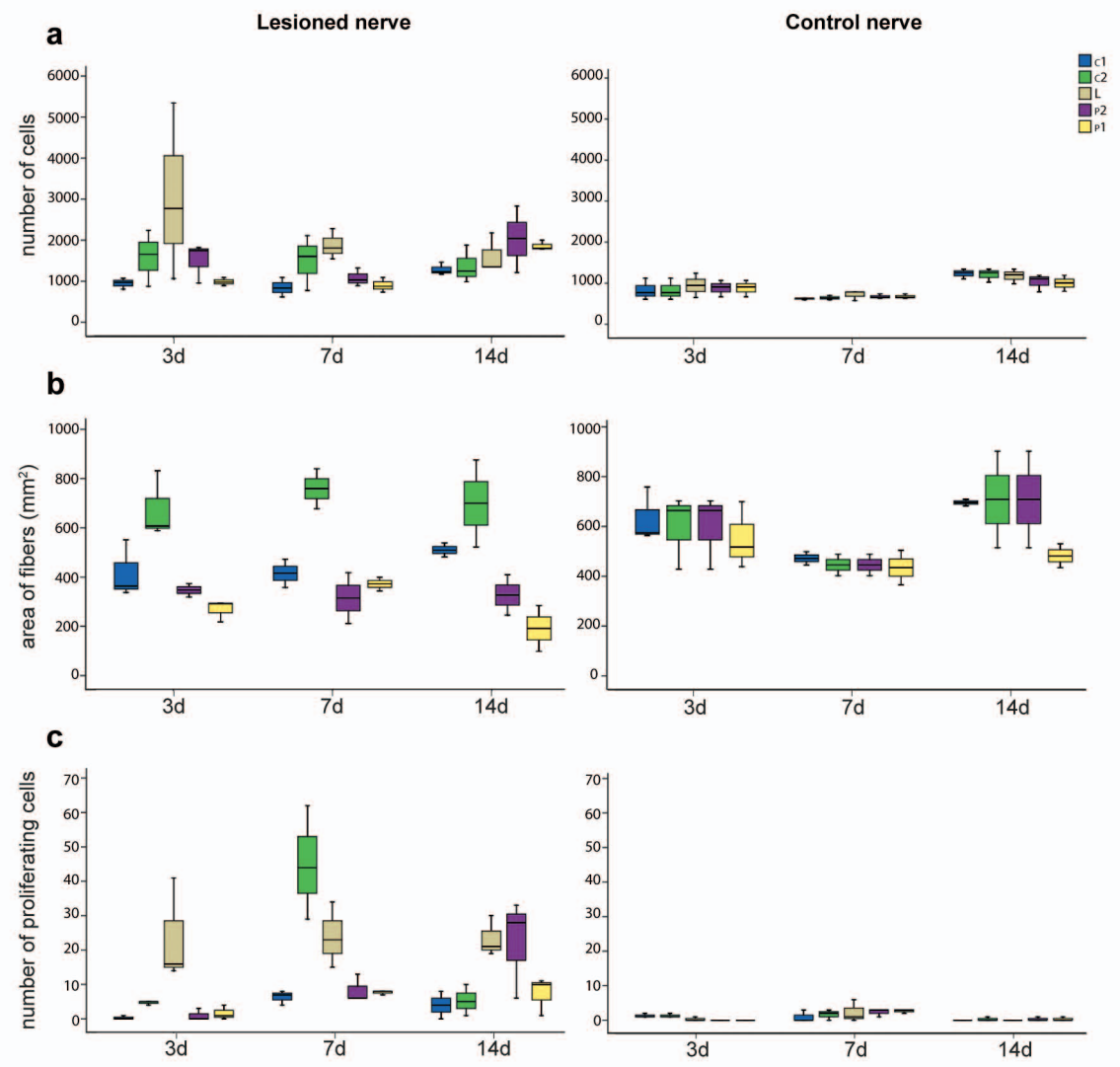
a
Lesioned nerve
Control nerve
c1
c2
L
p2
p1
number of cells
6000
5000
4000
3000
2000
1000
0
3d
7d
14d
b
area of fibers (mm²)
1000
800
600
400
200
0
c
number of proliferating cells
70
60
50
40
30
20
10
0

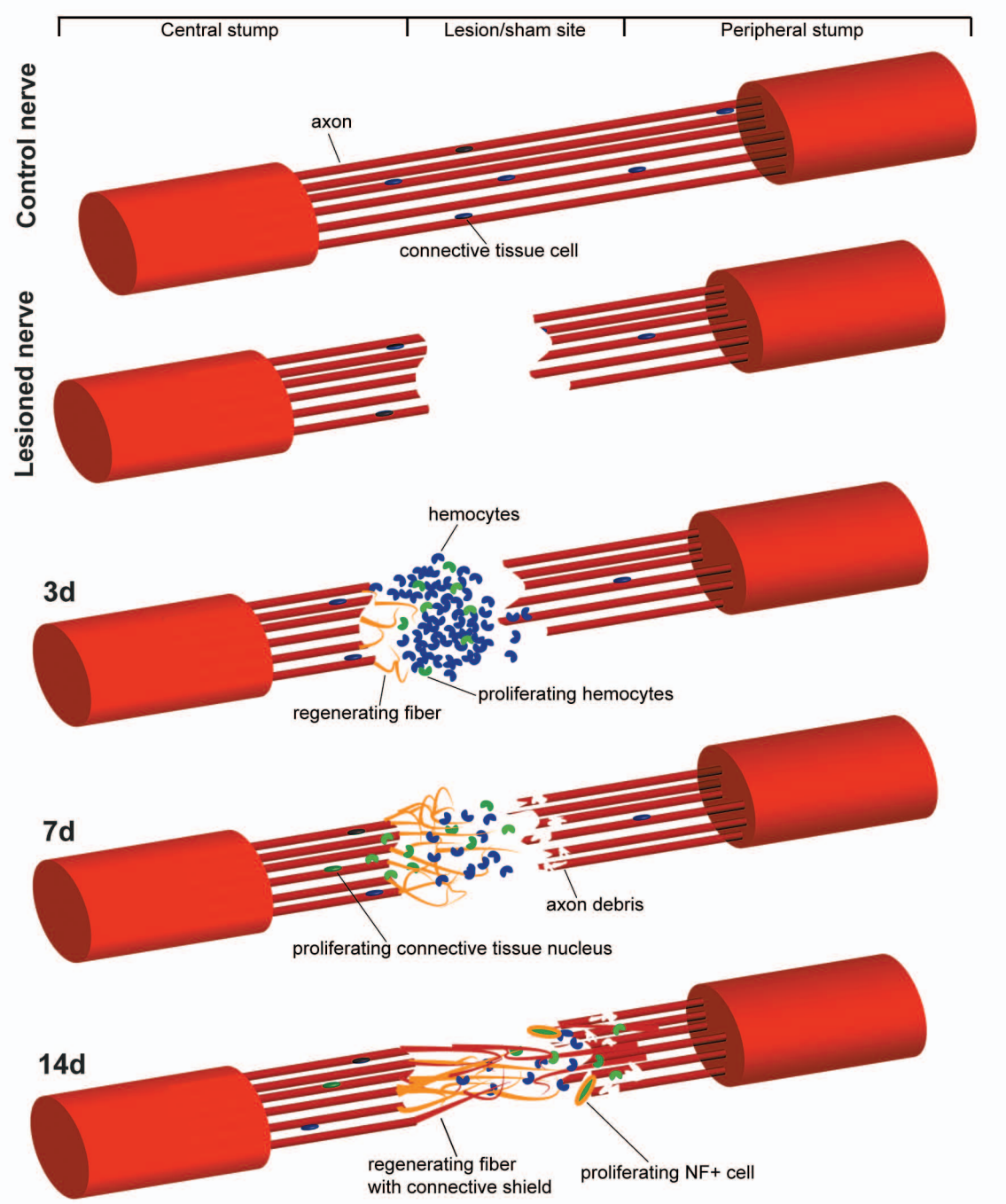
Central stump
Lesion/sham site
Peripheral stump
Control nerve
axon
connective tissue cell
Lesioned nerve
hemocytes
3d
proliferating hemocytes
regenerating fiber
7d
axon debris
proliferating connective tissue nucleus
14d
regenerating fiber
with connective shield
proliferating NF+ cell